WHOI-2002 - 10

Woods Hole Oceanographic Institution

A Comparison of Buoy Meteorological Systems

by

Richard E. Payne
Kelan Huang
Robert A. Weller
Woods Hole Oceanographic Institution

H. P. Freitag
M. F. Cronin
M. J. McPhaden
C. Meinig
NOAA Pacific Marine Environmental Laboratory

Yoshifumi Kuroda
Norifumi Ushijima
Japanese Marine Science and Technology Center

R. Michael Reynolds
Brookhaven National Laboratory

November 2002

Technical Report

Funding was provided by the National Oceanic and Atmospheric Administration under Grant Number NA96GPO429.

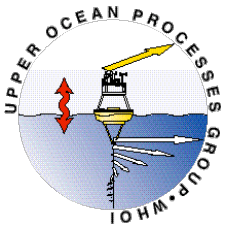

Upper Ocean Processes Group
Woods Hole Oceanographic Institution
Woods Hole, Massachusetts 02543

UOP Technical Report 02-05

Abstract

During May and June 2000, an intercomparison was made of buoy meteorological systems from the Woods Hole Oceanographic Institution (WHOI), the National Oceanographic and Atmospheric Administration (NOAA), Pacific Marine Environmental Laboratory (PMEL), and the Japanese Marine Science and Technology Center (JAMSTEC). Two WHOI systems mounted on a 3 m discus buoy, two PMEL systems mounted on separate buoy tower tops and one JAMSTEC system mounted on a wooden platform were lined parallel to, and 25 m from Nantucket Sound in Massachusetts. All systems used R. M. Young propeller anemometers, Rotronic relative humidity and air temperature sensors and Eppley short-wave radiation sensors. The PMEL and WHOI systems used R. M.Young self-siphoning rain gauges, while the JAMSTEC system used a Scientific Technology ORG-115 optical rain gauge. The PMEL and WHOI systems included an Eppley PIR long-wave sensor, while the JAMSTEC had no long-wave sensor. The WHOI system used an AIR DB-1A barometric pressure sensor. PMEL and JAMSTEC systems used Paroscientific Digiquartz sensors. The Geophysical Instruments and Measurements Group (GIM) from Brookhaven National Laboratory (BNL) installed two Portable Radiation Package (PRP) systems that include Eppley short-wave and long-wave sensors on a platform near the site.

It was apparent from the data that for most of the sensors, the correlation between data sets was better than the absolute agreement between them. The conclusions made were that the sensors and associated electronics from the three different laboratories performed comparably.

Table of Contents

List of Figures

(Pages 38–67)

Figure No.

List of Tables

1. Introduction

In the early 1990s, development of meteorological sensors for unattended use on moored buoys had progressed to the point that it was possible to make all of the measurements required to estimate the air-sea transfers of heat, fresh water, and momentum (Moyer and Weller, 1997). Extensive in-situ intercomparison of buoy and attended shipboard sensors during the TOGA COARE (Tropical Ocean-Global Atmosphere Coupled Ocean-Atmosphere Response Experiment) had demonstrated that such moored meteorological systems were capable of the accuracies needed to address questions of climate variability and air-sea interaction. Based on the success of COARE, plans have been developed for a sparse, international array of well-instrumented moored buoys that would serve as surface flux reference sites (Send et al., 2001). The success of such an array will depend on how well meteorological sensors from different laboratories can be intercalibrated and on their in-situ performance being comparable. To begin to address these issues, the Woods Hole Oceanographic Institution (WHOI), the Pacific Marine Environmental Laboratory (PMEL) of the National Oceanographic and Atmospheric Administration (NOAA), and the Japanese Marine Science and Technology Center (JAMSTEC) worked together to carry out a land-based comparison of the systems from the three laboratories. This report documents that comparison and the results.

The Upper Ocean Processes (UOP) Group at WHOI has been making observations of a complete suite of meteorological parameters from buoys in the deep ocean for approximately 15 years. Considerable effort has gone into making accurate measurements in order to compute momentum and heat fluxes through the ocean surface accurately. During the World Ocean Circulation Experiment (WOCE) the UOP Group at WHOI undertook an intensive effort to test, evaluate, and develop meteorological sensors for unattended use on ships and buoys, and also to develop low-powered electronics for moored meteorological systems (Hosom et al., 1995). The result was the IMET (Improved METeorological) system, with a family of sensor modules. For this land-based intercomparison, the UOP systems comprised IMET modules that were scheduled to be deployed later in the summer. Two sets of modules were mounted on a single buoy, standard UOP practice for redundancy.

PMEL began deploying buoys in the equatorial regions of the Pacific Ocean in the 1970s in order to monitor the conditions associated with the El Nino/Southern Ocean Oscillation (ENSO) cycle. That effort expanded through multi-national partnerships into the Tropical Atmosphere Ocean (TAO) Array spanning the entire equatorial Pacific basin (McPhaden et al., 1998). Beginning in 1996, PMEL developed an improved version of the original ATLAS (Autonomous Temperature Line Acquisition System), modified for higher sample rates, higher accuracy, and a more comprehensive suite of instrumentation (Milburn et al., 1996). This upgraded PMEL system, the Next Generation ATLAS, was used exclusively when PMEL expanded its efforts into the tropical Atlantic in collaboration with France and Brazil (Servain et al., 1998). Since November 2001 all moorings in the TAO array have been Next Generation ATLAS systems, which provide the option to include all the parameters needed for flux calculations (Cronin et al., 2002). The Next Generation ATLAS is the PMEL system used in this land-based intercomparison.

The JAMSTEC TRITON (TRIangle Trans-Ocean Buoy Network) (Kuroda and Amitani, 2001) buoy system comprises ASIMET (Air Sea interaction IMET) modules which are the latest generation of the IMET system. In 1998 JAMSTEC began replacing ATLAS buoys at some of the western positions of the TAO array with TRITON buoys. Their data are combined with the PMEL TAO array data to provide broad coverage of the equatorial Pacific Ocean in what is now referred to as the TAO/TRITON array.

This land-based experiment was designed to compare the integrated response of each institution's buoy-mounted meteorological system, including factors such as sensor performance, calibration procedures, digital processing, and in the case of the WHOI and PMEL systems, placement on the buoys. Performance issues related to at-sea conditions, such as buoy motion, are not addressed by this intercomparison.

1.1 Deployment

Table 1 summarizes the chronology of the intercomparison. Table 2 summarizes the data files yielded by the intercomparison, with the parameters recorded, the recording intervals, and start and stop times.

All buoy systems were mounted in a parking lot called Trunk River along the shore of Nantucket Sound near Woods Hole, Massachusetts. Figure 1 is a plan view of the parking lot and surrounding area. In this location the buoys could be lined up parallel to the shore, 4 m apart and approximately 27 m from the shore of Nantucket Sound. Figures 2-6 show the systems as they were deployed. Both of the WHOI systems were mounted on a single buoy; the two PMEL systems were on separate tower tops; and the JAMSTEC modules were mounted on posts on a wooden platform. A third set of WHOI sensors, not part of the intercomparison, can be seen in the background in Figure 2. The anemometers were all at the same altitude above the ground within 0.3 m. The local prevailing wind is approximately from the SW in the summer, but the directions experienced during the comparison covered all 360 degrees. From approximately105 to 225 degrees magnetic the wind approaches the beach over several miles of open water. Examination of the various parameters revealed no dependence on wind direction, so there was no discrimination between various wind directions. All directions in this report are magnetic with no magnetic variation applied.

The PMEL towers and the WHOI buoy were mounted so that the wind sensors were within 15 cm of each other vertically as determined by eye. The JAMSTEC sensors were mounted on posts attached to a wooden platform. The wind sensor was also lined up with the other wind sensors by eye and the remaining JAMSTEC sensors were mounted with the other sensors 0-30 cm below the anemometer level. Table 3 shows the sensor heights relative to the wind sensors.

The three buoy systems were in place at Trunk River from 5 May to 27 June. The first month was a shake-down period during which several problems were found with equipment. Several WHOI modules malfunctioned and the JAMSTEC system did not record high resolution data from 5 May to 2 June. Because of these problems, the comparison period for most parameters was 2-27 June. Between 17-23 June, the Rotronic sensors in the two WHOI systems

failed and were replaced. The relative humidity comparison omits this 6 day period. In the precipitation comparison, precipitation amounts were looked by event. Since there are so few events in the whole comparison period, all of them were used and the sensors that were working during each event were compared. On 8 and 21 June all vanes were tied down for several hours as a rough check on directions. On 9 June the two IMET wind modules were removed from their systems for several hours for direction checks in the laboratory. All three periods were omitted from the wind speed and wind direction comparisons. There is a four-day gap in the long-wave comparison during which the WHOI sensors were removed for calibration checks.

All three types of systems operated on batteries during the comparison and logged data internally, as well as transmitting a subset by satellite. All clocks were set to Universal Coordinated Time (UTC) with an accuracy of 5 s or better.

For an additional, and more accurate, determination of short and long-wave radiation, measurements were made from the roof of the Clark Laboratory about 300 m north of the Trunk River site and at an altitude of 55 m. UOP maintains a set of radiation sensors there recorded by a Campbell CR7 data logger. In addition, the Geophysical Instruments and Measurements Group (GIM) from Brookhaven National Laboratory (BNL) installed two Portable Radiation Package (PRP) systems, which include Eppley short-wave and long-wave sensors, at the Clark Laboratory facility.

Table 1

Chronology of buoy system intercomparison. YD is yearday of 2000.

YD	Date	Comment
115	24 April	PMEL systems 600 and 601 up and running on tower tops.
116	25 April	Leveled PMEL radiometers.
119	28 April	JAMSTEC system up and running on platform. PMEL towers rotated on platforms.
122	1 May	Remove both PMEL RH sensors.
123	2 May	Swap JAMSTEC Optical Rain Gauge for spare.
124	3 May	Lower JAMSTEC wind module to put all anemometers at the same level.
124	3 May	WHOI buoy moved to Trunk River.
125	4 May	WHOI buoy leveled.
126	5 May	Level all radiometers again.
131	10 May	BNL radiometers mounted on Clark Laboratory roof.
132	11 May	Newly calibrated RH sensors mounted on PMEL systems. All systems are complete.
140	19 May	BNL system 1 repaired.
154	2 June	JAMSTEC system restarted.
160	8 June	1710-2110 UTC, all vanes fixed in orientation. Directions observed with hand held compass.
161	9 June	WHOI wind modules removed from buoy for direction test.
165	13 June	1515 UTC, steady wind, observed all vane directions with hand held compass.
173	21 June	1515-2030. All vanes fixed in direction. Directions observed with hand held compass.

179	27 June	JAMSTEC system shut down and removed from platform.
181	29 June	WHOI buoy removed from Trunk River site.
182	30 June	Wind direction check of WHOI wind systems
187	5 July	PMEL systems removed from platforms.
187	5 July	Wind direction check of PMEL wind systems at WHOI
192	10 July	BNL systems removed from Clark Laboratory roof.

Table 2

Inclusive dates (year day/universal time, 2000) and recording intervals (RecInt) of basic data files. WS(windspeed), WD(wind direction), AT(air temperature), RH(relative humidity),BP(barometric pressure), SW(short-wave radiation), LW(long-wave radiation), PREC(precipitation)

Institution	**Parameters**	**RecInt**	**Begin** (YD/UTC)	**End** (YD/UTC)
PMEL	WS,WD,AT,RH	10 min	117/0800	181/1800
PMEL	BP	1 hr	117/0800	181/1800
PMEL	SWR,LW	2 min	117/0800	181/1700
PMEL	PREC	1 min	117/0801	181/1759
WHOI	WS,WD,AT,RH,SW, LW,PREC,BP	1 min	119/2000	181/1700
JAMSTEC	WS,WD,AT,RH,SW, PREC,BP	10 min	119/2110	126/1600
JAMSTEC	WS,WD,AT,RH,SW, PREC,BP	10 min	154/1620	179/1200
BNL	SW,LW	10 min	142/1620	192/1440

Table 3

Sensor Heights (m) relative to wind sensor

Sensor	PMEL	WHOI	JAMSTEC
Wind	0.0	0.0	0.0
BP	-1.6	-0.6	0.0
AT	-1.5	-0.7	-0.2
RH	-1.5	-0.7	-0.2
SWR	-0.5	+0.1	-0.3
LWR	-0.5	+0.2	No sensor
PRECIP	-0.5	-0.3	-0.1

1.2 Sensors

There is considerable similarity in the choice of sensors. All three systems used the R. M.Young Wind Monitor, although different shaft encoders were used by the three institutions in measuring wind direction (WD). All three used the Rotronic MP101 RH/AT sensor protected from solar radiation by an R.M.Young wind-aspirated shield. All three used the Eppley PSP pyranometer although the WHOI and JAMSTEC units used the WHOI-designed versions while the PMEL and BNL units used a PMEL-designed version of the sensors. WHOI and PMEL used Eppley PIR pyrgeometers, each with its own design modifications. JAMSTEC does not deploy a long-wave sensor. Eppley manufactures all versions to the specifications of each institution. The WHOI system uses the AIR DB-1A barometer, while PMEL and JAMSTEC use a Paroscientific Digiquartz sensor. WHOI and PMEL use the R. M. Young precipitation gauge, although PMEL has substituted their own internal electronics for the circuitry supplied by R. M.Young. JAMSTEC used the Scientific Technology ORG-115 optical rain gauge. Specifications of the sensors are given in Table 4.

Table 4
Range, accuracy and resolution of sensors

Parameter	WHOI Rng	WHOI Accy	WHOI Res	PMEL Rng	PMEL Accy	PMEL Res	JAM Rng	JAM Accy	JAM Res
WS(m s^{-1})	0.7-50	0.2 or 2%	0.1	1-20 (0.4-36)	0.3 or 3%	0.2	0-60	0.3	0.1
WD(deg)	0-360	2.8	0.7	0-359	5	1.4	0-360	10	1
AT(^{o}C)	0-35 (-40 to 45)	0.25	0.001	14-32 (0-40)	0.2	0.01	-20 to 55	0.2	0.01
RH(%RH)	20-95 (0-100)	2	0.1	25-95 (0-100)	2	0.02	28-95 (0-100)	4	0.1
BP(hPa)	950-1040 (850-1050)	1	0.1	800-1100	0.1	0.1	800-1100	0.02%	0.0038%
SW(W m^{-2})	0-1400	<10	0.1	200-1000 (0-1600)	1%	0.4	0-1400	6%	0.1
LW(W m^{-2})	0-600	<10	0.1	200 (±200)	2%	0.1			
PREC(mm)	0-50	1 cm/mo	1	0-50	0.4[2]	0.2[2]	0-500[2]	5%	0.001

1 - Measurement ranges listed are generally those over which the sensors are calibrated. The ranges over which a sensor will operate are listed in parenthesis if they differ significantly from the calibration range.
2 - units are mm hr^{-1}

1.3 Calibration

UOP sensors and modules are calibrated before and after each deployment. Where possible sensors and electronics are calibrated as a unit. Wind speed is not calibrated. It was found that the critical component of R.M.Young propeller anemometers is the propeller shaft bearings. These are replaced before each deployment. The differences between propeller calibration constants are very small (R.M.Young, personal communication) and less than the slight degradation of bearing performance during a year's deployment. Vanes and compasses are aligned before each deployment and checked after it. Digital barometers were compared with a Paroscientific Model 760 barometer and the constants in the sensor adjusted if the error was a bias or the sensor returned to the manufacturer for calibration if the error were more complex. Relative humidity sensors were calibrated with their electronics in a Tecnequip calibration chamber over the range 20-95 %RH. Chamber humidity was measured with a General Eastern Model 1500 dew point hygrometer. The air temperature sensor is an integral part of the relative humidity sensor and was calibrated with the module electronics in a Hart Model 7040 stirred water bath using an Azonix Model A1011 thermometer as a standard. Short-wave pyranometers were calibrated by The Eppley Laboratory, Inc. Long-wave pyrgeometers were calibrated using our own technique (Payne and Anderson, 1999). Electronics in both the long and short-wave modules were calibrated using high accuracy voltage and resistance standards. Precipitation gauges were calibrated with their module electronics by adding known amounts of water to the gauges.

ATLAS sensors are routinely calibrated before and after deployment, with most performed at PMEL. Wind speed sensors are calibrated in a PMEL wind tunnel by comparison with a standard sensor that is, in turn, traceable to the National Institute of Standards and Technology (Freitag et al., 2001). Wind direction sensors and compasses are also calibrated at PMEL (ibid). Air temperature sensors are calibrated in a PMEL temperature bath (Freitag et al., 1995). Relative humidity calibrations are performed at PMEL using a Thunder Scientific Corporation humidity chamber (Lake et al., in preparation). Short-wave pyranometers are calibrated either by the National Renewable Energy Laboratory, Golden, CO, or by the Eppley Laboratory, Inc., Newport, RI. The thermopiles in the long-wave pyrgeometers are also calibrated by the Eppley Laboratory, Inc. Nominal calibration coefficients are used for thermistors used in long-wave pyrgeometers. Rain gauges are calibrated at PMEL by measuring the sensor response to the addition of known volumes of water delivered by a precision pump. Digitization electronics for all sensors are calibrated either separately by applying precision laboratory voltage or resistance sources, or in combination during sensor calibrations. Accuracy for PMEL wind, air temperature, relative humidity and precipitation sensors listed in Table 4 are based upon analysis of field data and laboratory calibrations and tests (Freitag et al., 2001; Freitag et al., 1995; Lake et al., in preparation; Serra et al., 2001). Accuracy for PMEL barometric pressure, short and long-wave sensors is based upon manufacturers' specifications.

Most of the TRITON sensors are calibrated at JAMSTEC. Wind speed sensors are checked by driving the propeller shaft at a known rate with an R.M.Young Model 18801 anemometer drive at 500 rpm (corresponding to a wind speed of 2.45 m s^{-1}), 1000 (4.9), 3000 (14.7), 5000 (24.5), 7000 (34.3), and 9000 (44.1) and comparing with the module output. Propeller torque for starting rotation is checked with a torque meter to keep it within the

manufacturer-recommended value of 2.4 gm-cm. Wind direction sensors are calibrated by checking the output from an encoder in the ASIMET module with an encoder reader and adjusting to zero degrees before deployment, if necessary. After the encoder check, directions from the ASIMET module are checked in an outdoor calibration table before and after every deployment. The vane and compass are checked at 90 degree intervals in a clockwise direction and a counterclockwise one. Air temperature sensors are calibrated in a CTD calibration bath with a SBE-3 plus reference standard with seven points in the range 1º to 32ºC. Relative humidity sensors are calibrated at fifteen points in the 28.1 to 94.8%RH range using a Thunder Scientific Model 1500 humidity chamber. The humidity in the chamber is calibrated once per year by the Japan Quality Assurance Organization. Short-wave radiometers are calibrated using an artificial sun chamber (Ishikawa Trading Co., Ltd., model XC-500A with a 500 W xenon lamp) in the range from 50 W m^{-2} to 1350 W m^{-2} by varying the lamp-pyranometer separation distance. The reference radiometer, an Eppley PSP, is calibrated every two years at the Japan Meteorological Agency. The output signals of the optical rain gauge are checked using a tool provided by the manufacturer. Real water is not used for the calibration. Barometers are calibrated using a Ruska model 7010 digital pressure controller in the range from 880 hPa to 1025 hPa. Calibration constants in the ASIMET modules for wind speed and direction, air temperature and relative humidity, short-wave radiation, and barometric pressure are updated before deployment when the error exceeds the following values: 0.3 m s^{-1} in wind speed, 0.2 degrees in wind direction, 0.1º C in air temperature, 3%RH in relative humidity, 5% in short-wave radiation, and 0.02% in barometric pressure.

1.4 Sampling

The three meteorological systems employ different sampling and averaging schemes. These are described in Tables 5-7.

Table 5
WHOI sampling and recording.

Sensor	Sample Rate	Sample Period	Averaging Period	Data Recorded
Wind Vector		15 s	1 min	00:10:00
Speed	5 s integration			00:11:00
Vane	1 per 5 s			
Compass	1 per 15 s			
SW,LW,RH, AT,BP	1 per 5 s		1 min	00:10:00 00:11:00
PREC	1 per min		No averaging	00:10:00 00:11:00

Table 6
PMEL sampling and recording.

Sensor	Sample Rate	Sample Period	Sample Time	Data Recorded
Wind Vector	2 Hz	2 min	00:09-00:11	10 min
Speed	0.5 s integration		00:19-00:21	
Vane	2Hz			
Compass	2Hz			
SW, LW	1 Hz	2 min	00:01-00:03	2 min
			00:03-00:05	
RH, AT	2 Hz	2 min	00:09-00:11	10 min
			00:19-00:21	
BP	2 Hz	2 min	00:59-01:01	1 hour
			01:59-02:01	
PREC	1 Hz	1 min	00:01-00:02	1 min
			00:02-00:03	

Table 7
JAMSTEC sampling and recording

Sensor	Sample Rate	Sample Period	Sample Times	Data Recorded
Wind Vector		2 min	00:09-00:11, 00:19-00:21	10 min
Speed	5 s integration			
Vane	1 per 5 s			
Compass	1 per 5 s			
RH,AT	0.1 Hz	2 min	00:09-00:11, 00:19-00:21	10 min
SW	0.5 Hz	2 min	00:09-00:11, 00:19-00:21	10 min
PREC	0.2 Hz	10 min	00:00-00:10, 00:10-00:20	10 min
BP	1 per 10 min	no average	00:10, 00:20	10 min

Although the WHOI and JAMSTEC systems are both IMET, there is a fundamental way in which their data are recorded differently. The IMET modules return 1-minute averages when they receive the C command. WHOI systems record all the 1-minute values. The JAMSTEC systems average two of these 1-minute data each 10 minutes (unless there is only one taken). Also, due to differences between the generations of IMET modules, there is a difference in the way the 1-minute vector averages of wind speed and direction are computed. This is described in Section 2.

Figures 2-6 provide an overview of the installations used in the intercomparison study. Personnel from each of the laboratories came to Woods Hole to help with the installation and to start up and check their meteorological systems. During and subsequent to the field test, data was freely exchanged to facilitate the analysis.

1.5 Methods of Analysis

This experiment involved the comparison of similar sensors, but, in some cases, they have been modified, packaged, interfaced or calibrated differently by each laboratory. Because of this no single sensor was considered an absolute standard. In order to remove mean differences that were due to different calibration procedures or to imprecision in the calibrations, a reference time series was computed for each parameter that was the mean of all sensors (unless otherwise specified below). Individual time series were then "corrected" based on a linear least-squares fit to the reference series. The correction parameters that comprised a bias, A, and a slope, B, were applied by using equations of the form

$$X_{corrected} = A_X + B_X * X_{measured}$$

Where X represents a measured parameter, such as wind speed, wind direction, air temperature, etc. Differences between sensors were analyzed by computing the mean and standard deviations of differences between measured and reference time series ($X_{corrected}$-$X_{reference}$). By definition, mean differences between uncorrected time series (which are used in the reference) and the reference time series will sum to zero, and the mean difference between corrected and reference time series will be zero.

2. Wind Speed and Direction

Data were recorded with several sampling and averaging schemes:

WHOI – Anemometer counts (3 counts per propeller revolution, with one revolution per 29.4 cm of fluid displacement) summed for 5 s, vane read each 5 s, three speeds and compass value vector averaged to give 15 s speed and direction. Compass read each 15 s and combined with 15 s speed and direction to give 15s vector speed and direction. Four 15 s vectors vector averaged to give 1-minute vector, which is recorded.

PMEL – Anemometer counts (same resolution as for WHOI) summed for 0.5 s, vane and compass read each 0.5 s, vector computed for each 0.5 s set of values. Vectors summed over two-minute interval about 10 minute recording time.

JAMSTEC – Anemometer counts (same resolution as for WHOI) summed for 5 s, vane and compass read each 5 s, vector computed for each 5 s set of values. Eleven 5 s vectors summed to give 1-minute vector average. Two 1-minute averages about the 10-minute recording time and averaged together to give a 10-minute series. See section 2.2 for details on a firmware defect, which affected the wind computations.

WHOI wind speeds and directions were vector averaged to ten-minute series to provide a sample interval equal to that of PMEL and JAMSTEC.

2.1 Anemometer accuracy

R. M. Young selects the injection-molded propellers to be within 2% of their nominal calibration constant. They offer both unfilled and grease-filled stainless steel propeller shaft bearings. The grease-filled bearings have a higher threshold and a slightly lower calibration constant due to the drag of the grease. The IMET and ASIMET anemometers use a different bearing, unfilled but without the corrosion problems of the Young unfilled bearing. The grease-filled bearings used by PMEL have a higher threshold and a slightly lower calibration constant until they have run for a while and the grease gets evenly distributed. After that their characteristics are indistinguishable from the unfilled bearings (John Young, personal communication).

2.2 Direction checks

Prior to installation at the site near the beach, directions measured by each of the systems were checked at the site where the magnetic field is well known and where UOP routinely checks all its wind modules before deployment. A portion of the parking lot has been mapped to determine that the direction of magnetic north varies by less than 1 degree over the area. Vehicles are excluded from the area when direction checks are being done. The anemometer is aimed at a point ~100 m away and the wind unit rotated under it through 360 degrees with values of compass and vane and direction taken at 6-12 orientations. The magnetic direction of the point at which it is aimed is accurately known, so this provides a sensitive test of the direction measuring devices in each unit. Both PMEL units agreed with the known direction within 3 or 4 degrees at 12 or more different rotation positions. The two WHOI systems agreed with the known direction within ±2 degrees over 6 orientations. A similar test of the JAMSTEC unit was not done because of lack of time at the end of the experiment before the units had to be shipped back to Japan. Wind directions are all direction toward which the wind is blowing. All directions are relative to magnetic north (local magnetic variation is -15.8 degrees).

The IMET wind modules deployed in the UOP systems used a KVH Model C100 flux gate compass that has an accuracy of 0.5 degrees and a repeatability of 0.2 degrees. The ASIMET wind modules deployed in the JAMSTEC system used a Precision Navigation TCM2 magnetometer compass that has an accuracy of 0.5 degrees and a repeatability of 0.1 degrees.

For both compasses, accuracy degrades with tilt. This was not a concern in the comparison but is on a buoy at sea. For information on the PMEL compass, see Freitag et al., 2001.

While the systems were deployed at the beach, the vanes were tied down for two periods of a few hours each. During these periods the directions of each of the vanes were observed several time with a sighting compass. Also, during one period of unusually constant wind speed and direction, the direction of each vane was observed. None of these sets of observations had the precision of the parking lot check, but they did confirm that the directions returned by each of the systems agreed within ± 10 degrees, which was sufficient to show that they were roughly in agreement.

2.3 Comparison

Correction coefficients and statistics for uncorrected and corrected wind speed and direction time series are shown in Tables 8 and 9. By definition, a linear correction to a mean improves the mean difference but does not improve the standard deviation. The one exception is the JAMSTEC direction. The reason for this will be described later in this section.

Table 9 shows mean difference and standard deviation from the reference series for wind speed greater than 2 m s^{-1} because direction from the R.M.Young vane is most reliable above that speed.

Table 8
Wind Speed fit to reference series (mean of all 5).

System	A	B	Uncorrected Diff	Uncorrected SD	Corrected Diff	Corrected SD
	m s^{-1}		m s^{-1}	m s^{-1}	m s^{-1}	m s^{-1}
WH117	-0.02	0.997	0.03	0.40	0.00	0.43
WH226	-0.18	1.014	0.13	0.40	0.00	0.44
PM600	0.15	0.92	-0.06	0.33	0.00	0.36
PM601	-0.03	1.022	-0.04	0.28	0.00	0.33
JAM	0.08	0.996	-0.07	0.25	0.00	0.31

Figures 7A and 7C show mean (reference) wind speed and mean (reference) wind direction vs. time. The highest winds came from the east reaching values of 15 m s^{-1} in one brief period on June 6, although there were only a few speeds greater than 10 m s^{-1}, and 7 m s^{-1} on 13-14 June. Figures 7B and 7D show the differences between individual speeds and directions and their reference series. Most of the wind speeds are within ±1 m s^{-1} of the reference. The gap in speeds and directions on June 8 is during a period when the vanes were tied down. Direction differences in Figure 7D are plotted only when the speeds were greater than 2 m s^{-1}.

Table 9
Wind direction fit to reference series (WHOI and PMEL only).

System	A deg	B	Uncorrected Diff deg	Uncorrected SD deg	Corrected Diff deg	Corrected SD deg
WH117	-2.7	1.012	1.4	5.2	0.4	5.1
WH226	1.2	0.990	0.5	4.7	0.3	4.6
PM600	0.3	1.006	-1.0	4.3	0.0	4.3
PM601	1.0	0.998	-0.8	3.9	0.0	3.9
JAM	14.6	0.897	-0.5	14.0	-0.2	6.6

Figure 8A is an overplot of all the individual corrected speeds plotted against reference wind speed. A total scatter of about ±1 m s^{-1} about the 1:1 line is apparent. Figure 8B is the difference between individual corrected and reference speeds plotted against reference wind direction. There are two clusters of points. One, between about 40 and 75 degrees, corresponds to the nominal prevailing southwesterly breeze on Nantucket Sound in the summer. The other, between about 235 and 310 degrees, corresponds roughly to an easterly breeze. Figure 9A is a scatter plot of individual wind directions vs. reference wind direction, and Figure 9B is of wind direction minus reference direction vs. reference direction. In both plots a problem is apparent in the JAMSTEC direction.

The JAMSTEC wind directions had a problem due to a program defect in the ASIMET wind module firmware. In the corrected version, the module counts propeller revolutions for 5 seconds, reads the vane once each second and the compass once per 5 seconds. The mean vane for the 5-second interval is computed from the arc tangent of the quotient of the mean sine of the 5 angles and the mean cosine of the five angles. In the version used in the comparison, only the first four vanes were actually readings from the sensors. The fifth was retrieved from a location in memory, which stayed static. A simple model of the defect showed that the effect seen on Figures 9A and 9B can be reproduced by a constant fifth vane angle. Any fifth vane value gives a sinusoidal curve with a peak-to-peak amplitude of 30 degrees. Varying the fifth value merely shifts the curve along the *x* axis. This problem was corrected before the next deployment of ASIMET modules by JAMSTEC. Because of the problem, JAMSTEC wind directions were not used in computing the reference wind direction series.

The tide line on the beach has a direction of about 70 degrees magnetic. On the side of the parking lot opposite the water, there is about 100 m of salt marsh. From approximately SE through SW the wind approached the site over several miles of open water, an ideal situation. From the rest of the compass the wind approached the site over approximately 100 m of salt marsh and a pond. Examination of Figures 8B and 9B shows that there is no consistent increase

in scatter in any particular direction. From this it was decided that data from all directions could be used in this analysis.

Overall, the mean speeds agreed with each other within ±0.1 m s^{-1} and the directions within ±1 degrees. Doing a linear correction did not improve the scatter. Mean wind speed and direction differences with the reference series are much smaller than the specifications listed for each sensor in Table 4. Standard deviations are similar to those specifications for wind speed but in some cases larger than that specified for wind direction. This may be partially caused by the differences in the physical layout of the mountings of each of the three sets of sensors. Certainly the buoy configurations of the WHOI and PMEL buoys are quite different from each other and different from the platform on which the JAMSTEC sensors were mounted. There may also be differences in the turbulence seen by each sensor although the anemometer heights were carefully matched to within about 15 cm.

3. Relative Humidity and Air Temperature

All the systems used the Rotronic MP101A sensor to measure relative humidity (RH) and air temperature (AT) with the sensor elements protected by the Rotronic filter cap, which is made of expanded Teflon. This sensor has two voltage outputs: the RH channel outputs 0-1 VDC for a range 0-100%RH; the AT channel outputs 0-1 VDC for a 100°C temperature range, nominally –40° to 60°C for the sensors in this test. Manufacturer's repeatability specification is ±0.3% RH for relative humidity and ±0.1°C for air temperature. Humidity sensor stability is stated as better than 1% RH over 1 year. To the sensor error must be added the error due to heating by short-wave solar radiation. All the sensors were protected by R. M.Young Multiplate radiation shields. These rely on wind blowing through the plates to keep both the relative humidity and air temperature sensors at ambient air temperature. R. M.Young states that the heating of sensors in the shield at 1080 W m^{-2} short-wave radiation as 0.4°C @ 3 m s^{-1}, 0.7ºC @ 2 m s^{-1}, and 1.5ºC @ 1 m s^{-1}. Heating of the sensor will lead to indicated air temperatures, which are higher than actual ambient values and relative humidities, which are lower than the actual values. Since the buoy configuration was different for each institution, the effectiveness of the wind was different on each.

Figure 10A shows the ASIMET Rotronic sensor with the cap removed and the R.M. Young Multiplate radiation shield. Figure 10B shows the Rotronic sensor mounted in a R.M. Young shield in the ASIMET configuration. The three institutions use slightly different configurations of the R.M.Young Multiplate shield that lead to different lengths of the Rotronic sensor extending below the protection of the shield and different separations between the top of the Rontronic sensor and the lowest solid shield plate above it. The latter separations were all within the limits deemed acceptable by Richardson et al. (1999). The dimensions are shown on Figure 11, a sketch of the three sensor mountings. The total number of plates also differed. All three had three solid plates above the sensor, but the JAMSTEC (ASIMET) and WHOI (IMET) shields had 16 plates total and the PMEL shields had 12 plates total.

The basic Rotronic sensor has a time constant of approximately 10 s, but the filter cap increases the effective time constant to the order of minutes, its value being dependent on the wind speed and the sensor's exact position inside the shield.

3.1 Onsite calibrations

All five sets of air temperature/relative humidity sensors were recalibrated in the UOP calibration facility as an initial check that all calibration facilities were in agreement. JAMSTEC brought two ASIMET RH/AT modules, which had been calibrated at WHOI before being shipped to JAMSTEC upon their purchase in January 2000. The recalibration in April, before the deployment of one of them, agreed very well, within 0.05° C in temperature and 0.5% RH in humidity. The RH chamber used by PMEL for their calibrations has an absolute accuracy of ±0.5%RH while the dew point hygrometer used as a standard in the WHOI chamber has an accuracy of ±1.7%RH at 50%RH and ±3%RH at 95%RH. Since the 3% RH accuracy is only for the highest relative humidity values, it was assumed to have an overall calibration accuracy of ±2%RH. The calibrations at WHOI and PMEL of the PMEL sensors agree within the calibration and sensor accuracies and repeatabilities. WHOI and PMEL calibrations of the Rotronic temperature sensors agreed within 0.1°C.

3.2 Treatment of data

The WHOI 1-minute series were averaged to 10 minutes to coincide with the 2-minute PMEL and JAMSTEC averages, with the assumption that the difference in averaging period would not be significant for this comparison. Since calibrations are possible only to 95%RH and the sensors tend to be somewhat nonlinear at high values, ambient relative humidities close to, or at, 100%RH may be indicated as above 100%RH. Relative humidity values from some sensors indicated higher than 100%RH at times when the other RH sensors indicated high, but <100%, humidities. The JAMSTEC data logger automatically set relative humidity values indicated as greater than 100%RH to flagging characters (the data are excluded from the real time hourly averaging on the TRITON buoy in operation). At these times, the JAMSTEC air temperature data are also set automatically as flagging characters and linearly interpolated between the records immediately preceding and following the flagged records. The gap in RH comparison data from 17-23 June was due to a failure of the WHOI sensors.

There were two different major effects acting upon the accuracy of both the relative humidity and air temperature sensors. There were small differences in calibrations as were seen in all the other sensors but there were also differences in the degree of protection which the individual radiation shields gave to their sensors. The shield differences were apparent during the day while the calibration differences were predominant during the night. Accordingly, the analysis was divided into nighttime only, and complete 24-hour periods. JAMSTEC units had hard upper limits of 100%RH set in the recording section but this affected the data only slightly. The RH series were averaged together for all records for which the short-wave reference series had values of 10 W m^{-2} or less to compute the nighttime RH reference series. Since the linearly interpolated sections of the JAMSTEC air temperature were good approximations of the actual values, all five air temperature series were averaged together to compute the nighttime air temperature reference series.

Table 10 contains the values of the A and B constants derived for the nighttime series and the difference from the mean for RH and AT for corrected and uncorrected values and their standard deviations. The agreement is much better for both parameters after the correction has been applied. At minimum, this means that the stability of the sensors and electronics over a period of several months is better than our ability to calibrate them. Figures 12-13 show the nighttime data for RH and Figures 14-15 for air temperature. The improvement in agreement of RH is apparent in Figures 13A, 13B of uncorrected and corrected RH vs. reference RH as well as in Table 10. The change in air temperature through applying the corrections, Figures 15A and 15B, is slight.

The uncorrected nighttime temperature agreement is excellent, better than the basic accuracy of the sensor (0.3ºC as stated by the manufacturer). Uncorrected differences in relative humidity of up to 2%RH are to be expected, based on specifications of the instruments (Table 4). These results do not establish the absolute accuracy of the measurements but do show that all five systems agree to the degree that would expected, at least at night. These results confirm that our calibrations are equivalent within the accuracies of the sensors.

The same A and B correction constants were applied to the 24-hour data to obtain corrected series. These series are, thus, corrected only for calibration errors and still show the effects of short-wave radiation. For example, the mean differences between corrected and reference series are non-zero (Table 11).

Table 10

Nighttime relative humidity and air temperature fits to reference series (mean of all).

			Uncorrected		Corrected	
System	A	B	Diff	SD	Diff	SD
	%RH		%RH	%RH	%RH	%RH
WH 117	0.15	1.007	-0.76	0.87	0.00	0.87
WH 226	-1.72	1.047	-2.33	0.78	0.00	0.70
PM 600	-2.26	1.001	2.22	0.70	0.00	0.70
PM 601	2.83	0.955	1.26	1.30	0.00	1.17
JAM	0.81	0.995	-0.38	1.21	0.00	1.21

			Before correction		After correction	
	A	B	Mean	Std Dev	Mean	Std Dev
	ºC		ºC	ºC	ºC	ºC
WH 117	-0.09	1.003	0.04	0.05	0.00	0.05
WH 226	-0.14	1.007	0.04	0.06	0.00	0.06
PM 600	0.12	0.994	-0.02	0.06	0.00	0.06
PM 601	0.25	0.989	-0.08	0.08	0.00	0.07
JAM	-0.14	1.007	0.02	0.14	0.00	0.14

Table 11

24-hour relative humidity and air temperature fits to reference series (mean of all).

	Before correction		After correction	
System	Mean %RH	Std Dev %RH	Mean %RH	Std Dev %RH
WH 117	-0.53	1.15	0.19	1.14
WH 226	-1.99	1.04	0.07	0.88
PM 600	1.78	1.12	-0.44	1.13
PM 601	1.01	1.70	0.04	1.62
JAM	-0.27	1.22	0.14	1.22

24-hour air temperature fit to reference series (mean of all).

	Before correction		After correction	
	Mean °C	Std Dev °C	Mean °C	Std Dev °C
WH117	0.02	0.08	-0.01	0.08
WH226	-0.01	0.12	-0.04	0.12
PM600	0.06	0.14	0.08	0.13
PM601	0.08	0.22	0.15	0.19
JAM	-0.16	0.24	-0.17	0.23

The 24-hour relative humidity reference series in Figure 16 shows three periods when the relative humidity was close to saturation for periods of time of order a day, June 6-7, 12-13, and 16. All three events occur during cloudy weather as indicated on Figure 16D. The difference between individual RH values and the reference series in Figure 16B and 17A shows variations of order ± 4%RH and maximum differences during the periods of high humidity. The differences between corrected RH values and the references series in Figure 16C and 17B shows smaller values, of order ± 2%RH. The only wind event occurred during the high humidity values on June 6.

In Figures 17A and 17B the uncorrected and corrected values of relative humidity, respectively, are plotted against the reference RH. The correction makes a noticeable improvement, especially at values over 75%RH. In Figures 18A and 18B the difference between corrected RH values and the reference series are plotted against short-wave irradiance and wind speed respectively. There is no apparent dependence of the scatter of points on short-wave irradiance. Figure 18B indicates that the scatter may decrease with increasing wind speed but there are insufficient points at high wind speeds to make any quantitative estimates of the dependence.

Figure 19A shows the 24-hour reference air temperature series. The difference between uncorrected values and the reference series in Figure 19B and 20A shows substantial scatter

during periods of high short-wave irradiance. The amplitude of the scatter is not reduced in the corrected values, as shown in Figures 19C and 20B. Anomalies due to solar heating are positive for the PMEL sensors but negative for the WHOI and JAMSTEC sensors. This is to be expected since this is a difference relative to the average.

In Figures 21A and 21B the difference between corrected and reference values of temperature are plotted against short-wave radiation and against wind speed, respectively. The scatter of corrected values increases with increasing short-wave irradiance. There may be a dependence of scatter on wind speed although, as for relative humidity, there are not enough values at high wind speeds to make an estimate of the quantitative dependence.

4. Short-wave Radiation Flux

Data were recorded with several sampling and averaging schemes.

WHOI	- Records 1-minute averages starting on the minute
PMEL	- Records 2-minute averages centered on the even minute
JAMSTEC	- Records 2 minute averages centered on the 10 minutes.
BNL	- Records 2-minute averages starting on the even minute
Clark Roof	- Records 5-minute averages starting on the 5 minutes

All data series were recorded with UTC times except the Clark Laboratory roof unit, which was recorded with EST times, converted to UTC during processing. All systems used variations of the Eppley PSP pyranometer. The WHOI, JAMSTEC and Clark roof systems used a WHOI-designed version; the PMEL and BNL systems used a PMEL-designed version. The WHOI PSP on the roof of the Clark buildling was recorded on a Campbell CR7 data logger (CR7). The Brookhaven National Laboratory (BNL) radiometers were recorded on a BNL data logger (Reynolds and Bartholomew, 2001). The BNL (BNL1, BNL2) data showed nighttime biases of +3 to +12 W m^{-2}. Since the others all showed considerably smaller biases, the previous night's mean bias was subtracted from the succeeding day's values for both the BNL sensors. The WHOI sensors are denoted by WHOI117, WHOI226, and the PMEL sensors by PMEL600, PMEL601.

The Clark Laboratory is about 300 m north (away from Nantucket Sound) of the Trunk River site. UOP maintains a radiometer facility on the roof that has a clear view of the whole sky and amenities such as electric power. The radiometer facility is at an altitude of 55 m. The BNL units were mounted there because of the power availability, the excellent view of the sky, and the convenience of mounting.

4.1 Leveling

The PMEL and WHOI platforms were shimmed so that their pyranometers were within 0.5 degrees of horizontal as measured at the pyranometers. The JAMSTEC platform was leveled so that the pyranometer was within 0.6 degrees in the north-south plane and within 0.8 degrees in the east-west plane. The UOP pyranometer on the Clark roof was leveled within 0.1 degrees. All

leveling was done with a digital level. The BNL sensors were co-located on Clark roof with the WHOI PSP and were carefully leveled to ±0.2 degrees by BNL personnel.

In order to compare data from the different sources directly, the BNL, PMEL, and IMET data were averaged to 10 minutes. They were then combined to give a set of files containing only the days, June 3-26, when all the systems recorded data with no gaps. Figure 22A is an overplot of all the 10-minute series vs. time.

4.2 Comparison

Initial reviews of the data (Figure 22) showed significant differences between the short-wave time series. Dawn and dusk times were comparable but amplitude differences were evident. WHOI has found that the manufacturer's calibration can itself be uncertain. Thus, as with the other sensor types, calibration and performance issues were separated by making a linear regression fit of each of the raw (uncorrected) time series to a common reference time series. The reference 10-minute series was computed as the average of the two BNL series (corrected for night time bias) and the Clark roof CR7 series. These were chosen because they were leveled more precisely than it was possible to level the systems at the Trunk River site. Results of the difference analysis based on this reference are given in Table 12.

Table 12

Short-wave radiation fit to reference series (mean of BNL & CR).

System	A	B	Uncorrected		Corrected	
			Diff	Std Dev	Diff	Std Dev
	W m^{-2}		W m^{-2}	W m^{-2}	W m^{-2}	W m^{-2}
WH117	0.5	1.0400	-9.4	41.4	0.0	41.0
WH226	0.8	1.0420	-9.6	41.7	0.0	41.2
PM600	-0.3	1.0011	-0.6	28.8	0.0	28.8
PM601	0.0	1.0007	-0.2	30.4	0.0	30.4
JAM	0.1	1.0782	-18.6	48.1	0.0	45.0
BNL1	0.0	1.0075	-1.9	6.2	0.0	5.7
BNL2	0.4	0.9997	0.5	6.5	0.0	6.5
CR7	-0.4	0.9930	1.5	10.2	0.0	9.9

The effect of tilt on measured radiation depends on the amount and direction of tilt and the state of the sky. A solid overcast results in radiation approaching the sensor fairly uniformly from all parts of the sky. Small tilts will result in very little error in these cases. In a clear sky when most of the radiation is coming from the direction of the sun the effect of tilt is maximized. A tilt to the east or west will change the apparent time of solar noon but will effect the daily total radiation very little. In Northern Hemisphere mid-latitudes a tilt to the north will decrease apparent radiation while a tilt to the south will increase it. In addition, very detailed calibrations of pyranometers (none of which have been published in the scientific literature) indicate that there are variations in pyranometer sensitivity with both altitude and azimuth of the radiation

source relative to the pyranometer. On a buoy, these concerns are inconsequential since the sensor is continually in motion about the horizontal and, indeed, the attitude of the sensor cannot be defined at any time. Correction for the tilt could not be calculated because the distribution of radiance about the sky was not known. However, the buoy systems of all three institutions use taut line moorings with high tensions in the mooring lines. An assessment of the effect of environmental conditions on moored short-wave radiation measurements is given by Medavoya (1999) and Medavoya et al. (2002). Measurements of the tilt of WHOI buoys a few years ago yielded amplitudes of only a few degrees.

The JAMSTEC short-wave radiation indicated 8% lower than the BNL reference data. Pre-calibration of the pyranometer at JAMSTEC indicated it read 4% lower than a reference sensor of the JAMSTEC calibration facility. The JAMSTEC data were not corrected for this difference. The purpose of JAMSTEC calibration is to ensure calibration traceability. If the calibration difference had been applied to the JAMSTEC comparison data, the mean difference with the reference time series and its standard deviation would have been similar to those of the WHOI sensors. The other 4% may be caused by some difference between the calibration techniques or calibration reference sensors. It may be useful to intercompare the calibration reference sensors at some point in the future.

Figures 23A and 23B are overplots of all series vs. the reference series for the uncorrected and corrected data, respectively. The agreement is noticeably better after correction. This indicates that the sensors may be better than the calibration of the sensors and electronics and that better leveling would very likely have improved the agreement.

Figure 24A is an overplot of differences between uncorrected 10-minute values and the reference during June 4, a day exceptionally free of clouds and, therefore, a maximum amount of direct radiation. It would be expected that any poor leveling would show up in this plot. It shows:

1. The standard deviation of BNL, PMEL600 and Clark roof PSP differences are within about 10 W m^{-1} of the mean all day and have no apparent tilt relative to each other. Since the BNL and Clark roof sensors comprise the reference series, they would be expected to agree well.

2. The WHOI117, WHOI226, and JAMSTEC sensors are tilted toward the north, leading to underestimates of the irradiance; and,

3. The PMEL601 sensor is tilted toward the east.

Figure 24B is an overplot of differences between uncorrected 10-minute values and the reference during June 6, a very cloudy day. Since the irradiance is nearly all diffuse, it would be expected that slight tilting of the sensors have little effect and that the corrected values would agree well. The figure shows that this is, indeed, the case.

4.3 Daily Means

For many studies, daily averages are of more value than 10-minute averages. Table 13 shows the uncorrected daily averages for all sensors for each of the comparison days as well as

the mean and standard deviation over all sensors. The all-sensor mean was used in order to contrast cloudy sky with clear sky response.

The day with the most clouds and least bright periods was June 6. The averages for that day agree within 1 W m^{-2} with the mean over all eight values indicating that, without the problems of tilting platforms, the agreement is quite good, about 2%. Eppley does not state an overall accuracy for the PSP. Eppley states that the temperature dependence is within 1% over –20 to +40ºC, the linearity is ± 0.5 % from 0 to 2800 W m^{-2}, and the cosine response is within 1% from the vertical to 30 degrees above the horizon within 3% from 10 to 20 degrees above the horizon.

The standard deviation about the mean of the three reference sensors (BNL1, BN2, CR7) is below 1% except on the three cloudy days. That the standard deviation of all the sensors about the daily overall is several times larger is because of the imperfect leveling of the buoy-mounted sensors.

Table 13

Daily averages of shortwave radiation in W m^{-2}

	WH117	WH226	PM600	PM601	JAM	BNL1	BNL2	CR7	Mean	SD	%SD	MeanRef	RefSD	%SD
June 3	345.0	345.8	358.4	358.4	333.5	354.3	358.2	358.8	351.6	9.3	2.6	357.1	2.4	0.7
June 4	356.2	356.1	368.9	369.4	342.2	367.8	371.3	371.5	362.9	10.5	2.9	370.2	2.1	0.6
June 5	278.7	277.9	294.4	294.7	274.5	295.0	296.9	297.2	288.7	9.8	3.4	296.4	1.2	0.4
June 6	30.7	30.5	30.1	31.0	29.6	30.2	31.7	31.3	30.6	0.7	2.2	31.1	0.8	2.5
June 7	189.6	190.7	203.4	201.1	195.6	191.6	194.7	193.9	195.1	4.9	2.5	193.4	1.6	0.8
June 8	282.1	284.8	293.4	298.9	266.5	294.5	301.5	301.4	290.4	12.0	4.1	299.1	4.0	1.3
June 9	254.8	257.1	267.0	269.5	247.4	267.4	269.2	272.1	263.1	8.8	3.4	269.6	2.4	0.9
June 10	327.2	326.4	339.8	339.5	315.1	337.6	341.2	342.4	333.7	9.7	2.9	340.4	2.5	0.7
June 11	261.8	263.2	277.0	279.4	255.0	274.2	277.0	279.3	270.9	9.4	3.5	276.8	2.6	0.9
June 12	49.2	48.7	50.8	50.5	48.0	51.0	50.5	53.4	50.3	1.7	3.3	51.6	1.6	3.0
June 13	268.5	264.0	273.4	273.1	249.5	272.2	273.2	276.0	268.7	8.6	3.2	273.8	2.0	0.7
June 14	216.2	213.2	220.0	219.4	206.0	223.6	226.0	225.4	218.7	6.8	3.1	225.0	1.2	0.6
June 15	51.1	50.6	52.6	52.7	49.6	54.8	55.7	55.8	52.9	2.4	4.5	55.4	0.6	1.0
June 16	303.4	301.7	312.9	310.3	295.1	308.4	310.7	312.5	306.9	6.3	2.0	310.5	2.1	0.7
June 17	314.6	315.1	326.8	327.5	302.3	325.4	328.5	329.8	321.3	9.7	3.0	327.9	2.3	0.7
June 18	192.7	195.1	199.6	202.6	181.2	201.6	202.3	205.0	197.5	7.8	3.9	203.0	1.8	0.9
June 19	205.3	205.3	209.7	212.7	198.6	210.0	209.7	213.3	208.1	4.8	2.3	211.0	2.0	0.9
June 20	342.7	343.0	355.0	355.3	327.7	354.3	358.7	356.6	349.2	10.6	3.0	356.5	2.2	0.6
June 21	304.4	303.4	316.1	316.0	294.4	315.6	318.5	318.7	310.9	9.0	2.9	317.6	1.7	0.5
June 22	173.0	169.3	167.1	166.5	157.4	164.1	165.6	166.0	166.1	4.5	2.7	165.2	1.0	0.6
June 23	330.0	331.2	343.2	342.3	317.6	339.8	343.6	344.4	336.5	9.5	2.8	342.6	2.5	0.7
June 24	320.2	323.3	334.6	335.1	309.3	334.0	335.8	338.3	328.8	10.2	3.1	336.0	2.2	0.6
June 25	326.9	325.3	335.7	334.8	312.4	334.4	337.3	337.4	330.5	8.6	2.6	336.4	1.7	0.5
June 26	213.6	212.9	220.2	219.6	211.1	216.7	217.6	219.3	216.4	3.4	1.6	217.9	1.3	0.6

5. Long-wave Radiation

Data were recorded with several sampling and averaging schemes.
WHOI - Records 1-minute averages on the minute
PMEL - Records 2-minute averages centered on the even minute
BNL - Records 2-minute averages on the even minute

For the purposes of this comparison all series were averaged to 10 minutes. All systems used variations of the Eppley PIR pyrgeometer. The WHOI system used a WHOI-designed version; the PMEL systems used a PMEL-designed version. The BNL PIR design was similar to the PMEL and BNL PSPs. The WHOI sensors are denoted by WHOI117, WHOI226; the PMEL sensors by PMEL600, PMEL601; and the BNL sensors by BNL1, BNL2. The JAMSTEC system did not include a long-wave sensor.

5.1 Leveling

The PMEL and WHOI platforms were shimmed so that their radiometers were within 0.5 degrees of horizontal as measured at the radiometers. All leveling was done with a digital level. The BNL sensors were co-located on the Clark roof with the WHOI PSP and were carefully leveled by BNL personnel to within ±0.2 degrees. It was discovered after the comparison that the WHOI sensors had a problem, which resulted in anomalously high thermopile voltages, especially at night.

5.2 Comparison

Therefore, for comparison purposes, an average of the two PMEL and the two BNL series was computed to form a reference series. Figure 25A shows the reference time series. Figure 25B is a plot of all six long-wave measurements. It is apparent that there are times when the sensors are definitely sensing the conditions differently. Computing a mean over all the values at each record time would not have provided a meaningful basis of comparison. Table 14 shows the results of fitting all six sets of data to the reference series.

Table 14
Long-wave radiation fit to reference series (mean of PMEL & BNL).

			Before correction		After correction	
Sensor	A	B	Bias	SD	Bias	SD
	W m^{-2}		W m^{-2}	W m^{-2}	W m^{-2}	W m^{-2}
PM600	-8.1	1.0231	2.1	2.2	0.0	2.1
PM601	-16.5	1.0373	3.0	2.5	0.0	2.2
BNL1	23.4	0.9423	-2.8	4.7	0.0	4.2
BNL2	11.7	0.9736	-2.3	2.9	0.0	2.8
WH117	-14.8	1.0392	0.7	10.3	0.0	10.3
WH226-	13.0	1.0086	9.8	12.8	0.0	12.8

Figures 26A and 27A show the uncorrected and corrected WHOI series plotted against the reference series. The linear correction does improve agreement with the reference series but does not eliminate the anomalous values. The problem appears to be a generic one with the WHOI sensors and probably has affected previous deployments.

Figures 26B and 27B show the uncorrected and corrected long-wave values from the BNL and PMEL systems plotted against the reference long-wave series. It is apparent that a linear correction does improve the agreement between them.

5.3 Daily Means

As for short-wave irradiance, daily means of long-wave irradiance are significant for many studies. Table 15 shows the uncorrected daily averages for all sensors for each of the comparison days. The means are taken over only the PMEL and BNL sensors because of the anomalous behavior of the WHOI sensors. Over these four, the agreement is very good with standard deviations of 2-5 W m^{-2}. The effect of the anomalous behavior is particularly noticeable in WH226 where the daily averages depart from the mean by up to 26 W m^{-2}.

6. Precipitation

Both the WHOI and PMEL systems used R. M. Young capacitative rain gauges. However, PMEL has replaced the internal electronics provided by R. M.Young with their own design that generates a frequency inversely proportional to the volume of water in the gauge. The frequency is counted each second and summed by a low power microprocessor. The master logger requests a sample every minute and the rain gauge responds by sending back the total integrated frequency count and the number of one second samples. When the level reaches approximately 50 mm, the gauge self-siphons. In the WHOI system, the output voltage is recorded at 1-minute intervals. The difference in level between two consecutive times then gives the total precipitation in that interval (taking into account, of course, any fillings and self-siphonings which took place) and, thus, the rain rate. The JAMSTEC system used a Scientific Technology ORG-115 optical rain gauge, which outputs a voltage proportional to rain rate. To determine the total precipitation, one sums the rain rates for all the intervals in the time of interest. To compare them, a time series was generated for each consisting of the total accumulated precipitation vs. time. Figure 28A is a time series plot of the accumulated precipitation amounts. Since there were only three rain events during the designated comparison period for the other meteorological sensors, all the events were looked at during the whole period when the systems were operating at Trunk River, 29 April to 30 June. Figure 28B shows the wind speed through the comparison period.

6.1 Comparison of eight rain events

Table 16 gives the total precipitation recorded by each gauge for the eight events. The WHOI117 gauge was not operating during the first event and the JAMSTEC system recorded

only during the last three events. The mean is computed only for the WHOI and PMEL gauges. The WHOI and PMEL gauges agree very well for all but the event that began on 6 June. The wind speed was greater than 10 m s^{-1} for the first 11 hours of the event on 6-7 June. Figures 29A and 29B show the rain rates and wind speed during the first event. During the other events the wind speed never exceeded 5 m s^{-1}. Since the R.M.Young rain gauge tends to underestimate precipitation in high winds (Yuter and Parker, 2001), it is likely that the different mounting configurations on the WHOI and the PMEL buoys, leading to different effects of the wind, are

Table 15

Daily averages of uncorrected long-wave irradiance (W m^{-2})

					(REF is mean of PMEL & BNL)					
Date	**PM600**	**PM601**	**BNL1**	**BNL2**	**REF**	**SD**	**WH117**	**DIFF**	**WH226**	**DIFF**
5/24	365.7	366.0	360.2	362.8	363.7	2.4	360.2	-3.5	371.3	7.6
5/25	346.6	346.8	348.1	344.2	346.4	1.4	346.4	0.0	357.4	11.0
5/26	312.4	313.9	303.8	307.5	309.4	4.0	310.5	1.1	321.7	12.3
5/27	309.2	310.1	299.6	303.9	305.7	4.2	307.4	1.7	318.1	12.4
5/28	328.9	329.3	319.2	324.2	325.4	4.1	324.4	-1.0	334.4	9.0
5/29	322.6	322.8	313.3	319.3	319.5	3.8	321.4	1.9	330.9	11.4
5/30	330.7	330.7	319.7	328.5	327.4	4.5	330.3	2.9	339.9	12.5
5/31	319.5	324.1	310.9	313.0	316.9	5.2	318.7	1.8	333.0	16.1
6/1	358.0	359.2	352.6	357.0	356.7	2.5	355.1	-1.6	367.5	10.8
6/2	359.3	360.3	351.4	356.4	356.8	3.5	356.2	-0.6	367.1	10.3
6/3	343.0	344.3	344.0	338.5	342.5	2.3	340.7	-1.8	351.6	9.1
6/4	296.3	298.5	289.0	290.8	293.7	4.5	307.0	13.3	319.4	25.7
6/5	334.0	335.3	326.4	330.4	331.5	4.0	330.6	-0.9	342.2	10.7
6/6	373.1	373.1	366.8	370.3	370.8	3.0	366.2	-4.6	377.3	6.5
6/7	345.8	346.4	345.5	339.1	344.2	3.4	341.2	-3.0	353.4	9.2
6/8	319.7	322.0	311.9	314.0	316.9	4.7	331.1	14.2	343.2	26.3
6/9	350.9	351.3	343.4	345.6	347.8	3.9	347.5	-0.3	359.2	11.4
6/10	359.0	360.3	351.8	355.2	356.6	3.8	356.6	0.0	367.9	11.3
6/11	354.5	355.5	351.3	350.6	353.0	2.4	353.4	0.4	365.3	12.3
6/12	369.9	369.8	377.6	365.5	370.7	5.0	363.6	-7.1	374.9	4.2
6/13	356.2	357.4	349.9	352.3	354.0	3.5	352.3	-1.7	366.3	12.3
6/14	365.2	365.9	358.3	361.6	362.8	3.5	360.6	-2.2	371.9	9.1
6/15	387.2	387.2	379.5	384.5	384.6	3.6	381.4	-3.2	392.1	7.5
6/16	385.0	386.0	382.3	382.8	384.0	1.8	381.4	-2.6	393.6	9.6
6/17	380.6	381.3	378.8	377.6	379.6	1.5	376.1	-3.5	388.7	9.1
6/18	379.6	380.0	373.4	375.0	377.0	2.9	373.9	-3.1	383.5	6.5
6/19	394.6	394.4	390.7	391.5	392.8	1.7	388.8	-4.0	398.8	6.0
6/23	360.6	363.0	354.2	355.6	358.4	3.6	360.0	1.6	356.5	-1.9
6/24	346.7	347.9	336.2	339.1	342.5	5.0	349.9	7.4	347.3	4.8
6/25	360.2	361.4	350.4	353.0	356.3	4.7	368.7	12.5	365.8	9.5
6/26	409.6	409.8	407.6	406.0	408.3	1.6	409.6	1.4	408.0	-0.3
6/27	399.6	400.3	394.7	395.4	397.5	2.5	400.3	2.8	400.9	3.4
6/28	374.4	375.4	378.1	367.1	373.8	4.1	373.9	0.1	372.1	-1.6

responsible for the large discrepancies during the this event. The size of the differences at these wind speeds is disturbing, however, and indicates that caution should be used when evaluating rainfall recorded at wind speeds >10m s^{-1}. It is possible that the WHOI measurements could be improved by changing the position of the gauge on the buoy. In low wind speed conditions, the standard deviations about the mean for each of the gauges are within the accuracy of the R. M. Young gauge, stated by the manufacturer as ±1 mm.

In a test of the ORG-115 at a JAMSTEC land site, seven ORG sensors indicated larger values (by factors of 1.07 to 1.34) than a reference tipping bucket rain gauge (Kawahara et al., 2001). Bradley et al. (2001) state that ORG gauges record larger amounts than other gauges. In this comparison, the JAMSTEC ORG recorded substantially smaller amounts than the R. M. Young gauges. Therefore, the gauge used in the comparison may have had a malfunction.

Table 16

Precipitation accumulation by event

Total amounts and differences from mean of WHOI and PMEL gauges

Date Time Begin	**Date Time End**	**Total event precip in mm**									
		WH117		**WH226**		**PM600**		**PM601**		**Mean**	**JAM**
5/10 1500	5/10 1840	25.1	0.5	23.4	-1.2	25.1	0.5	24.6	0.0	24.6	
5/1 0250	5/11 0800	5.3	-0.1	5.6	0.2	4.8	-0.6	6.0	0.6	5.4	
5/1 0020	5/20 2000			9.6	-0.3	9.5	-0.4	10.5	0.6	9.9	
5/23 0130	5/23 0830			8.9	0.1	8.7	-0.1	8.7	-0.1	8.8	
5/24 1210	5/24 1630	21.5	-1.2	20.5	-2.2	23.6	0.9	24.9	2.2	22.7	
6/2 2240	6/3 0400	7.5	-0.5	8.6	0.6	8.2	0.2	7.6	-0.4	8.0	1.4
6/6 1210	6/7 1400	16.7	-4.1	18.0	-2.8	24.2	3.4	24.1	3.3	20.8	12.3
6/11 2000	6/12 1700	17.3	0.9	16.2	-0.2	15.2	-1.2	19.8	3.4	16.4	3.7
RMS Difference			1.8		1.4		1.4		1.9		

7. Barometric Pressure

The sensors used by each institution and their accuracies as specified by the manufacturer are listed in Table 4. All three systems use a form of the Gill (1976) pressure port, designed to minimize the effects of wind past the pressure inlet.

7.1 Comparison

Hourly averages were computed for the WHOI and JAMSTEC data to give record times coincident with the PMEL record times. The WHOI files were averaged over sixty 1-minute values, the JAMSTEC over six 10-minute values, and the PMEL represented a two-minute average. A mean over the five values was computed for each hourly record as well as the difference from the mean for each BP.

Mean difference and standard deviation from the reference series computed from all of the five series are shown in Table 17. Because differences were very small, no linear least-squares fit to a reference time series was performed.

Table 17
Pressure differences (hPa) and standard deviations from reference (mean of all)

	WH117	WH1226	PM600	PM601	JAM
Mean Difference	0.008	-0.003	0.029	0.032	-0.066
Standard Deviation	0.05	0.04	0.04	0.04	0.04

Figure 30A shows the hourly barometric pressure averaged over the five sensors as a function of time. Figure 30B is an overplot of all the differences from the mean. The scatter increases on June 6 when the wind (Figure 30C) rises to more than 10 m s^{-1}, showing that either the ports are not equally effective or that the wind speed is substantially different at the various ports. It is also possible that, since there are periods on June 6 when the pressure is changing rapidly, that some of the differences are due to sampling. It is apparent, however, that all the sensors agree very well and are within manufacturer's specifications.

For a strict comparison, the WHOI and JAMSTEC data should not have been averaged before being compared with the PMEL data. Since the WHOI and JAMSTEC systems transmit hourly averages while the PMEL transmits hourly samples, the comparison was carried out as described to see if there was any advantage to either scheme. The results indicate that hourly sampling is equivalent to averaging for the sensors deployed and the conditions encountered.

8. Conclusions

It was found, with some exceptions, that the sensors and associated electronics from the three different laboratories performed comparably. However, it is quite evident that attention to calibration, development of better calibration methods and standards, and development of the means to assure cross-calibrations and repeatability are still needed. This was demonstrated by the frequent need to do a linear fit of raw sensor data to a common reference in order to remove the first order differences. On the positive side, the improvement in agreement achieved in many cases by this procedure indicates that calibration uncertainties are a major source of error. In principle, this is something that could be improved with no improvements to the sensors themselves. In addition, it was learned that three different laboratories could prepare, calibrate, and field surface meteorological systems that agreed well and that, with attention to calibration and continuing sensor development and improvement (especially for long-wave radiation), the goal of "interchangeable climate quality" data is attainable.

For several of the sensor types the following additional conclusions were reached:

1. **Wind speed and direction**. Differences in speed before correction were 0.1 m s^{-1} or less. Standard deviation between individual anemometer speeds and the reference speed was 0.4 m s^{-1}. Uncorrected mean direction differences were in the range of ±1.4 degrees. The standard deviation of direction differences was 4°-5°, except for the JAMSTEC sensor that had a direction problem that has since been corrected. This agreement reassures us that all three laboratories are taking care with possible magnetic and other influences.

2. **Relative humidity and air temperature**. The radiational heating problem is well known, but it is unclear why the different systems showed differences in radiational heating. The small differences in the configurations of the radiation shields could possibly be responsible. For relative humidity, it is evident that there are uncertainties in calibration which lead to differences of typically 2% RH. After correction, however, performance was good with small standard deviations of less than 1% RH across the range of humidities. Especially reassuring was the good agreement of the corrected humidities at and above 90% RH. Some of the differences observed in RH could be the result of differences in air temperatures inside the shields stemming from the different shield configurations.

3. **Short-wave radiation**. In addition to calibration uncertainties, attention to leveling was critical. The standard deviation about the mean of all sensors was several times that of the three precisely leveled reference sensors. For buoys, this will be a challenge. Uncorrected daily averages agreed with approximately 3% of the all-sensor means. See Table 13.

4. **Long-wave radiation.** In addition to calibration uncertainty for all long-wave radiation sensors, both WHOI sensors had time-dependent differences, which require further study. Mean differences between individual sensors and the reference series were 3 W m^{-2} or better for the PMEL and BNL sensors and one of the WHOI sensors. The second WHOI sensor had a mean difference of 10 W m^{-2}. See Table 14.

5. **Precipitation**. The performance of the optical rain gauge was not good, consistent with literature reports. However, the R. M. Young siphon gauges used by PMEL and WHOI agreed, for the most part, within the specified accuracy of the gauge, ±1 mm. The largest differences occurred during the 10 m s^{-1} wind event and may be due to the different aerodynamics of the system configurations.

6. **Barometric pressure**. The sensors all had excellent agreement, within 0.05 hPa in the mean. No significant instrumental issues were raised. Under the conditions encountered in this comparison, equivalent time series were produced by either hourly samples or hourly averages.

Acknowledgements

WHOI
The WHOI facilities group set up the Trunk River site. Bryan Way prepared the WHOI IMET modules and the tower. WHOI participation was funded by NOAA contract NA96GPO429.

PMEL
We thank Andy Shepherd, Pat McLain and Patrick A'Hearn for the preparation and installation of ATLAS instrumentation as well as data processing and assessment. PMEL participation in this project was supported by NOAA's Office of Oceanic and Atmospheric Research.

JAMSTEC
We thank Koichi Takao, Atsuo Ito and Takeo Matsumoto of Marine Works Japan Ltd (MWJ) for the preparation and deployment of the equipment for the comparison test, Tetsuya Nagahama of MWJ for the calibration of the TRITON sensors, and Kentaro Ando, Yasushi Takatsuki and Toru Nakamura of JAMSTEC for the valuable comments on TRITON data quality in an early version of this report. The Japanese Ministry of Education, Culture, Sports, Science and Technology supported the TRITON project as part of which the JAMSTEC could participate in the comparison.

References

Bradley, E. F., R. A. Lukas and S. de Carlo, 2001. A fresh look at rainfall estimates during TOGA-COARE. Proceedings Workshop on Air-Sea fluxes, 21-25 May 2001, Potomac, MD, WCRP.

Cronin, M.F., N. Bond, C. Fairall, J. Hare, M.J. McPhaden, and R.A. Weller, 2002. Enhanced oceanic and atmospheric monitoring underway in the eastern Pacific. *EOS, Transactions, AGU*, **83**(19), p 205, 210-211.

Freitag, H.P., Y. Feng, L.J. Mangum, M.J. McPhaden, J. Neander, and L.D. Stratton, 1995. Calibration procedures and instrumental accuracy estimates of TAO temperature, relative humidity and radiation measurements. NOAA Tech. Memo. ERL PMEL-104, 32 pp.

Freitag, H.P., M. O'Haleck, G.C. Thomas, and M.J. McPhaden, 2001. Calibration procedures and instrumental accuracies for ATLAS wind measurements. NOAA Tech. Memo. OAR PMEL-119, NOAA/Pacific Marine Environmental Laboratory, Seattle, Washington, 20 pp.

Gill, G., 1976. Development and testing of a no-moving-parts static pressure inlet for use on ocean buoys. University of Michigan Report.

Hosom D. S., R. A. Weller, R. E. Payne and K. E. Prada, 1995. The IMET (Improved Meteorology) ship and buoy systems. *Journal of Atmospheric and Oceanic Technology,* **12,** 527-540.

Kawahara, M., K. Ando, Y. Kuroda and Y. Takatsuki, 2001. Land site test of optical rain gauge used on TRITON buoy. *JAMSTECR*, **43**, 25-35 (in Japanese with English abstract).

Kuroda, Y. and Y. Amitani, 2001. TRITON: New ocean and atmosphere observing buoy network for monitoring ENSO. *Umi no Kenkyo*, **20**, No. 2, 157-172 (in Japanese with English abstract).

Lake, B.J., S. Noor, H.P. Freitag, and M.J. McPhaden. Calibration procedures and instrumental accuracy estimates of ATLAS air temperature and relative humidity measurements. NOAA Tech. Memo. In preparation.

McPhaden, M.J., A.J. Busalacchi, R. Cheney, J.R. Dinguy, K.S. Gage, D. Halpern, M. Ji, P. Julian, G. Meyers, G.T. Mitchum, P.P. Niiler, J. Picaut, R.W. Reynolds, N. Smith, and K. Takeuchi, 1998. The Tropical Ocean-Global Atmosphere (TOGA) observing system: A decade of progress. Jo*urnal of Geophyiucal. Research*, **103**, 14,169-14,240.

Medavoya, M., 1999. A method for assessing the integrity of ocean buoy shortwave observations under operation conditions. MS Thesis, State University of New York at Stony Brook, Stony Brook, NY, 95 pp.

Medavoya, M., D.E. Waliser, R.A. Weller and M.J. McPhaden, 2002. Assessing ocean buoy shortwave observations using clear-sky model calculations. *Journal of Geophysical Research*, **107**, 3014, DOI 10.1029/2000JC000558.

Milburn, H.B., P.D. McLain, and C. Meinig, 1996. ATLAS buoy-reengineered for the next decade. In: Proceedings of IEEE/MTS Ocean'96, Fort Lauderdale, FL, September 23-26, 1996, 698-702.

Moyer, K. A. and R. A. Weller, 1997. Observations of surface forcing from the Subduction experiment: A comparison with global model products and climatological data sets. *Journal of Climate,* **10,** 2725-2742.

Payne, R.E., and S. Anderson, 1999. A new look at calibration and use of Eppley Precision Infrared Radiometers. Part II: Calibration and use of the Woods Hole Oceanographic Institution improved meteorology precision infrared radiometer. *Journal of Atmosphere and Oceanic Technology,* **16**, 739-751.

Reynolds, R.M., and M.J. Bartholomew, 2001. Radiation measurements by Brookhaven National Laboratory during the Woods Hole Oceanographic intercomparison study—May-June 2000. Brookhaven National Laboratory report BNL-52609, 37pp. Brookhaven National Laboratory, Upton, NY 11973.

Richardson, S. J., F. V. Brock, S. R. Semmer, C. Jirak, 1999. Minimizing errors associated with multiple radiation shields. *Journal of Atmosphere and Oceanic Technology,* **16,** 1862-1872.

Serra, Y.L., P. A'Hearn, H.P. Freitag, and M.J. McPhaden, 2001. ATLAS delf-siphoning rain gauge error estimates. *Journal of Atmospheric and Oceanic Technology*, 18, 1989-2002.

Servain, J., A.J. Busalacchi, M.J. McPhaden, A.D. Moura, G. Reverdin, M. Vianna, and S.E. Zebiak, 1998. A pilot research moored array in the tropical Pacific (PIRATA). *Buletin of the American Meteorological Society*, **79**, 2019-2031.

Send, U., R. Weller, S. Cunningham, C. Eriksen, T. Dickey, M. Kawabe, R. Lukas, M. McCartney, and S. Osterhus, 2001. Oceanographic timeseries observatories. In: *Observing the Oceans in the 21st Century*, C. J. Koblinsky and N. R. Smith, editors, GODAE Project Office, Bureau of Meteorology, Melbourne, Australia, pp.376-390.

Yuter, S. E. and W. S. Parker, 2001. Rainfall measurement on ship revisited: The 1997 PACS TEPPS cruise. *Journal of Applied Meteorology*, **40**, No. 6, 1003-1018.

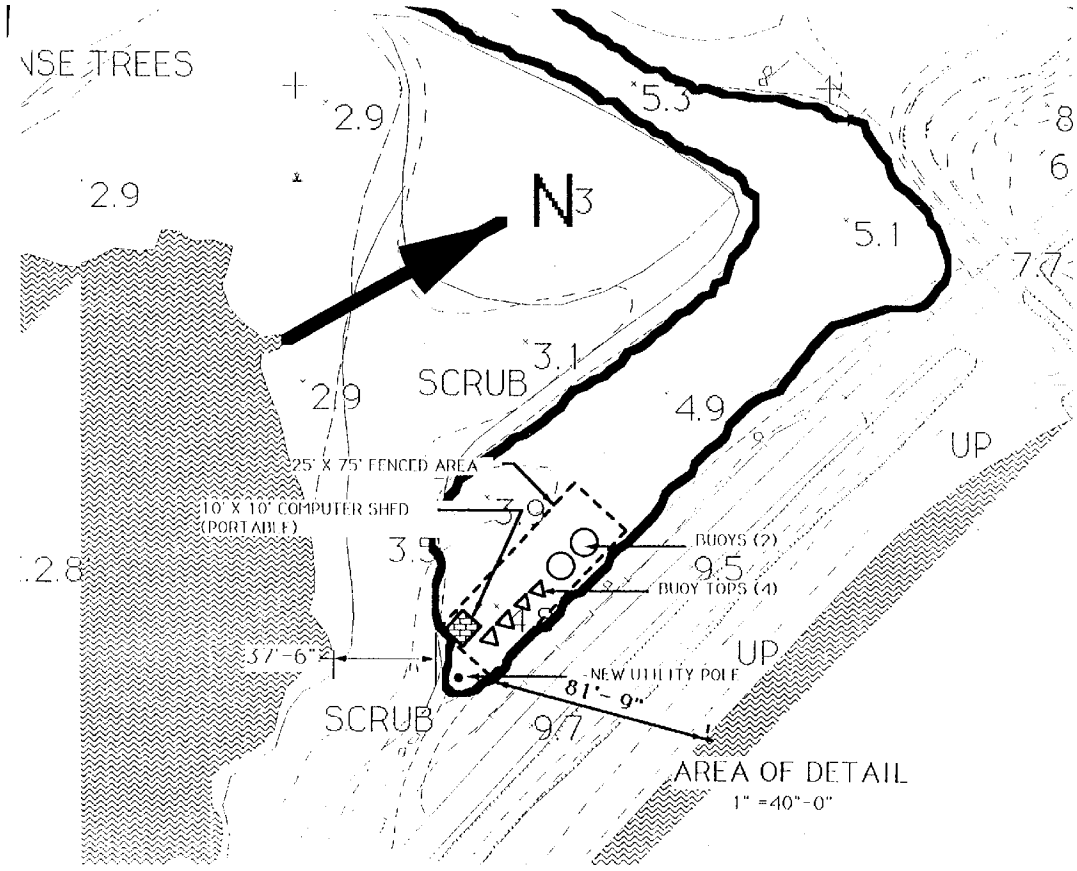
NSE TREES
2.9
5.3
2.9
N
5.1
7.7
SCRUB
3.1
2.9
4.9
UP
25' X 75' FENCED AREA
10' X 10' COMPUTER SHED
(PORTABLE)
3.9
BUOYS (2)
9.5
BUOY TOPS (4)
37'-6"
NEW UTILITY POLE
81'-9"
UP
SCRUB
9.7
AREA OF DETAIL
1" =40'-0"

Figure 1

Figure 2

Figure 3

Figure 4

Figure 5

Figure 6

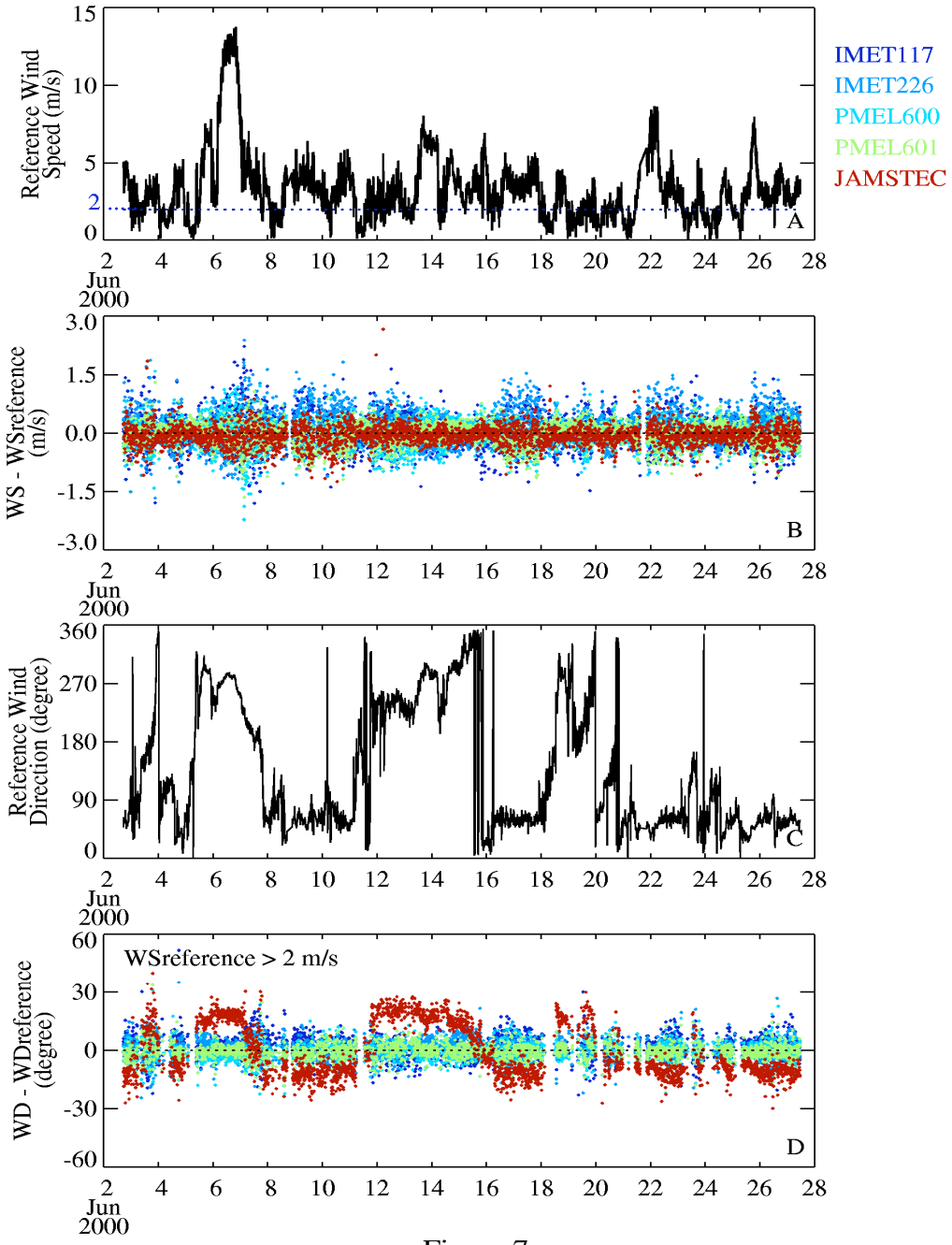
IMET117
IMET226
PMEL600
PMEL601
JAMSTEC
Reference Wind Speed (m/s)
A
WS - WSreference (m/s)
B
Reference Wind Direction (degree)
C
WD - WDreference (degree)
WSreference > 2 m/s
D
Jun 2000

Figure 7

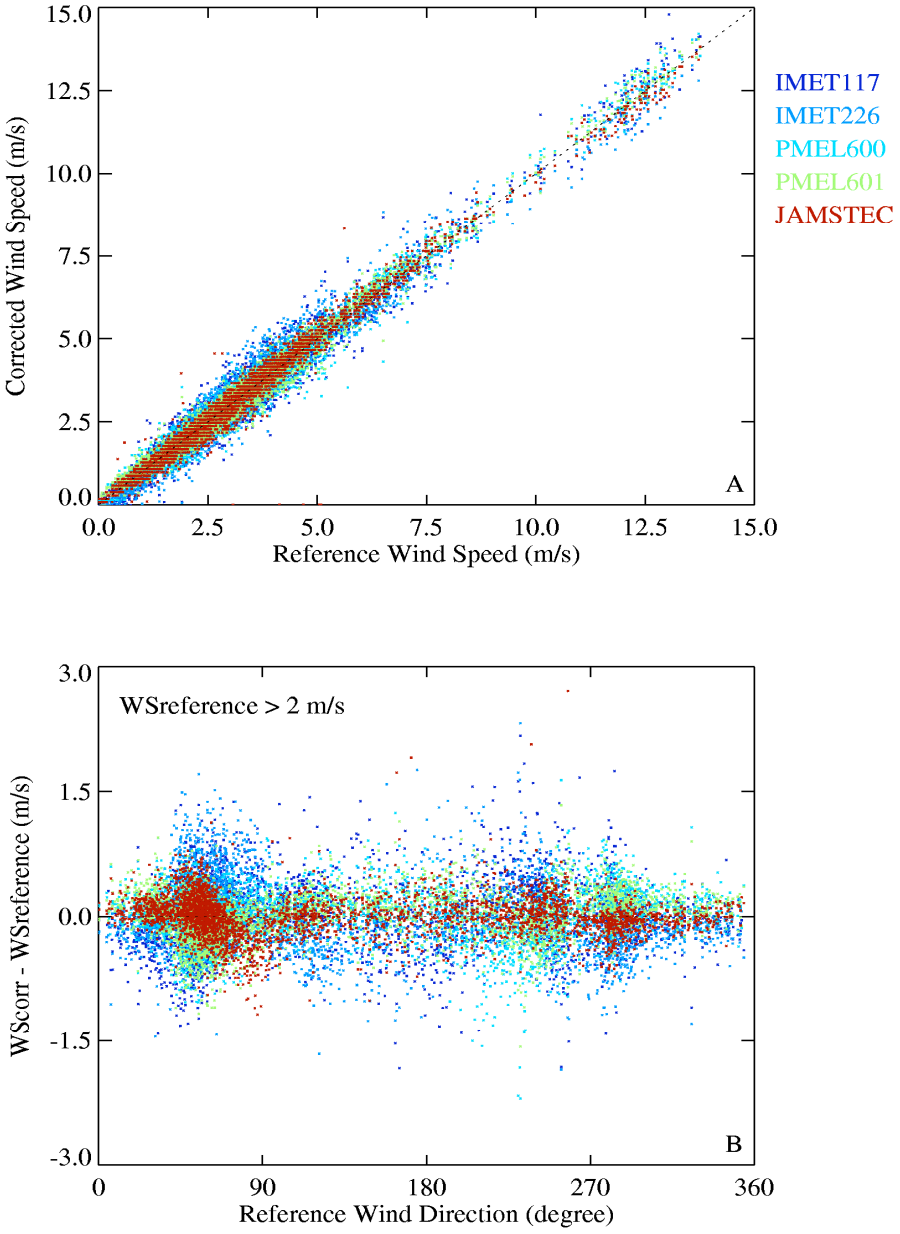
15.0
12.5
10.0
7.5
5.0
2.5
0.0
Corrected Wind Speed (m/s)
0.0
2.5
5.0
7.5
10.0
12.5
15.0
Reference Wind Speed (m/s)
A
IMET117
IMET226
PMEL600
PMEL601
JAMSTEC
3.0
1.5
0.0
-1.5
-3.0
WScorr - WSreference (m/s)
WSreference > 2 m/s
0
90
180
270
360
Reference Wind Direction (degree)
B

Figure 8

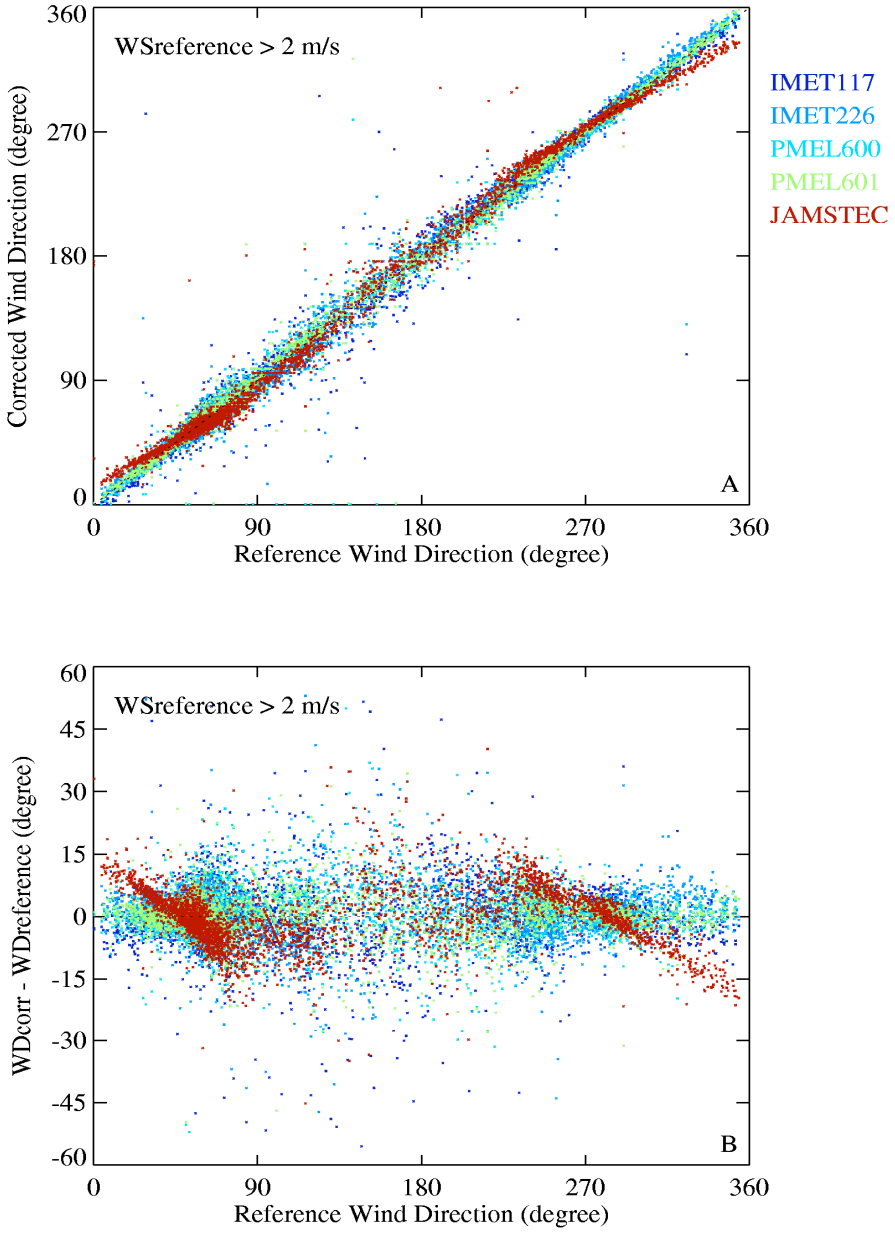
WSreference > 2 m/s
Corrected Wind Direction (degree)
Reference Wind Direction (degree)
A
IMET117
IMET226
PMEL600
PMEL601
JAMSTEC
WSreference > 2 m/s
WDcorr - WDreference (degree)
Reference Wind Direction (degree)
B

Figure 9

Figure 10

Figure 11

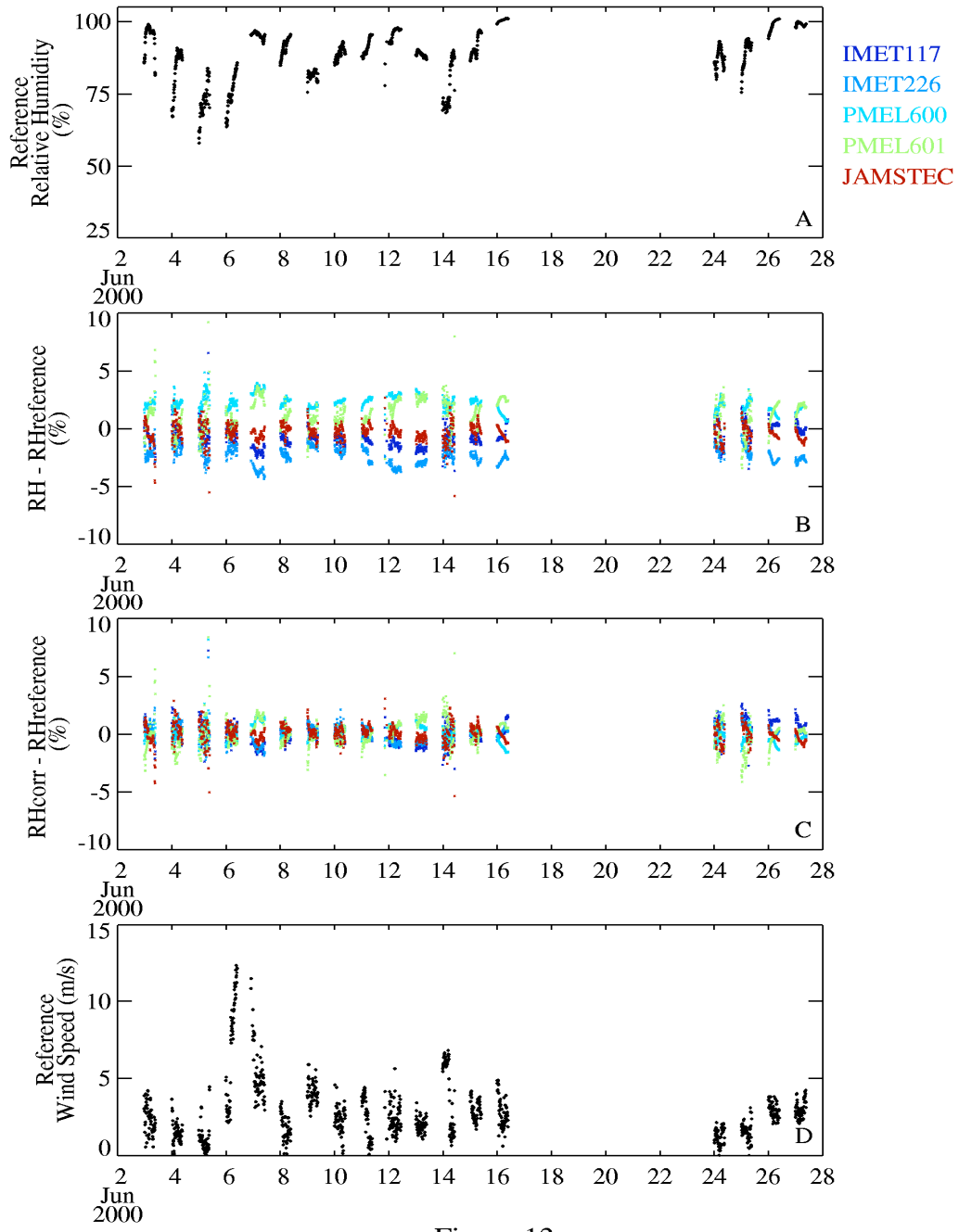
Reference
Relative Humidity
(%)
100
75
50
25
A
IMET117
IMET226
PMEL600
PMEL601
JAMSTEC
2
4
6
8
10
12
14
16
18
20
22
24
26
28
Jun
2000
RH - RHreference
(%)
10
5
0
-5
-10
B
RHcorr - RHreference
(%)
C
Reference
Wind Speed (m/s)
15
D

Figure 12

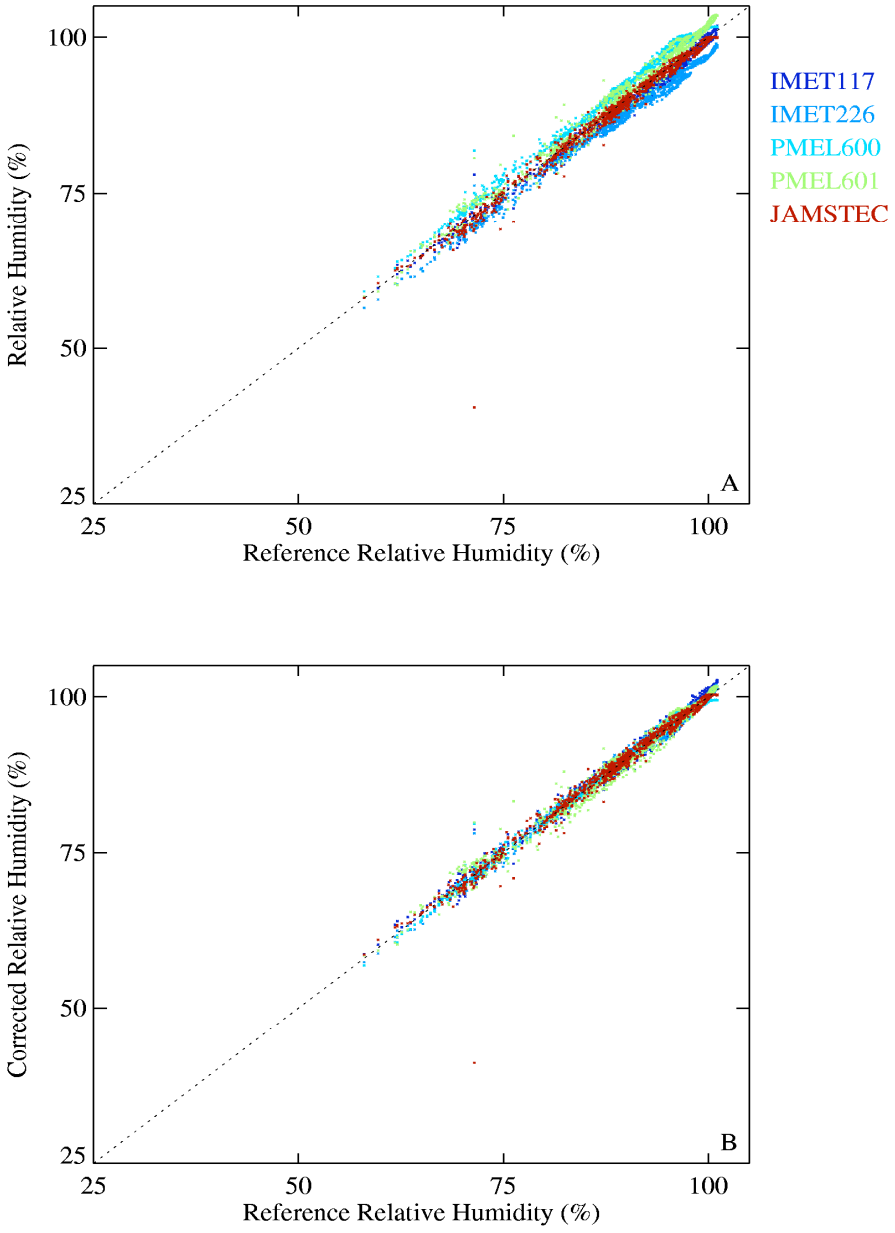
100
75
50
25
Relative Humidity (%)
25
50
75
100
Reference Relative Humidity (%)
A
IMET117
IMET226
PMEL600
PMEL601
JAMSTEC
100
75
50
25
Corrected Relative Humidity (%)
25
50
75
100
Reference Relative Humidity (%)
B

Figure 13

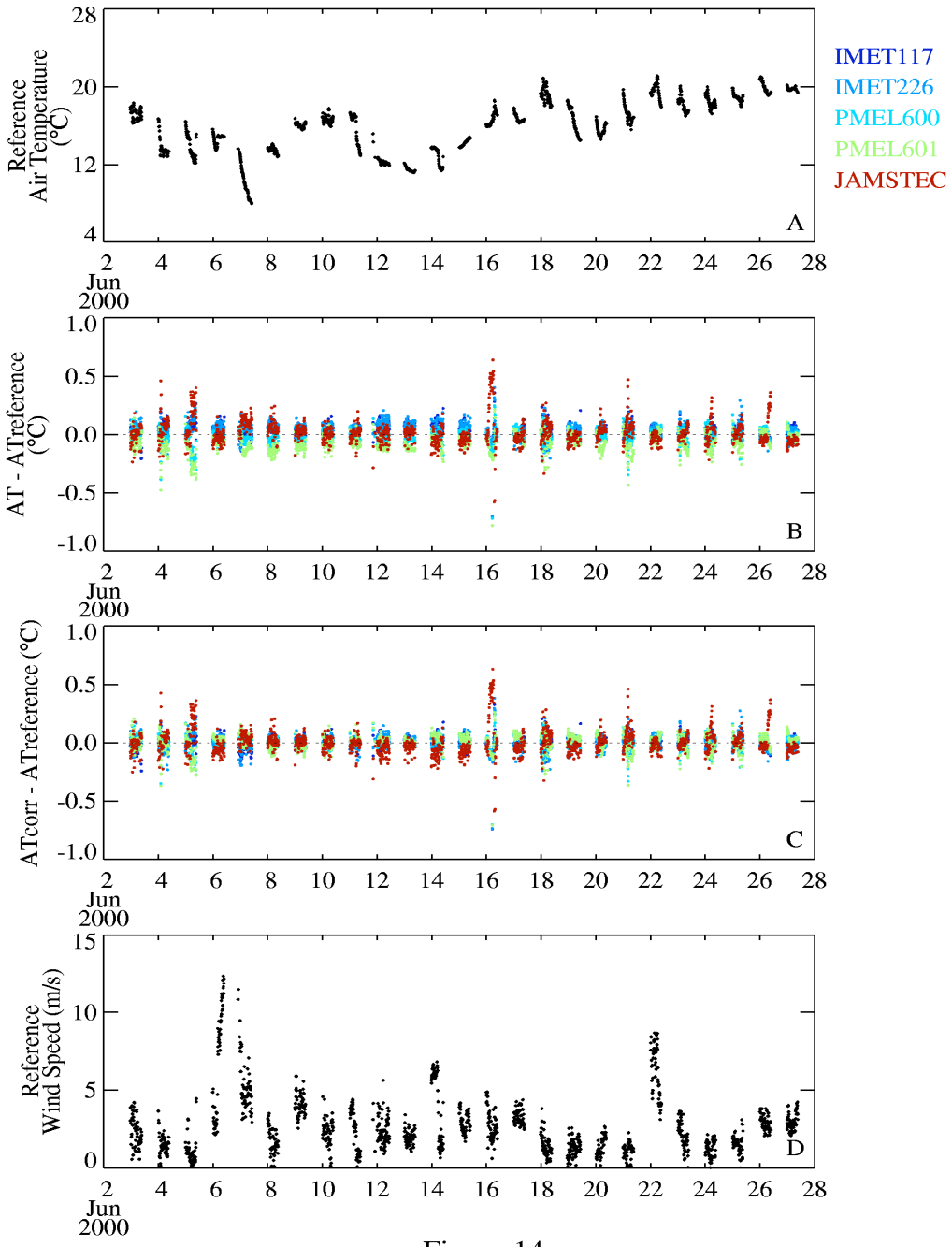
IMET117
IMET226
PMEL600
PMEL601
JAMSTEC
Reference Air Temperature (°C)
A
AT - ATreference (°C)
B
ATcorr - ATreference (°C)
C
Reference Wind Speed (m/s)
D
Jun 2000

Figure 14

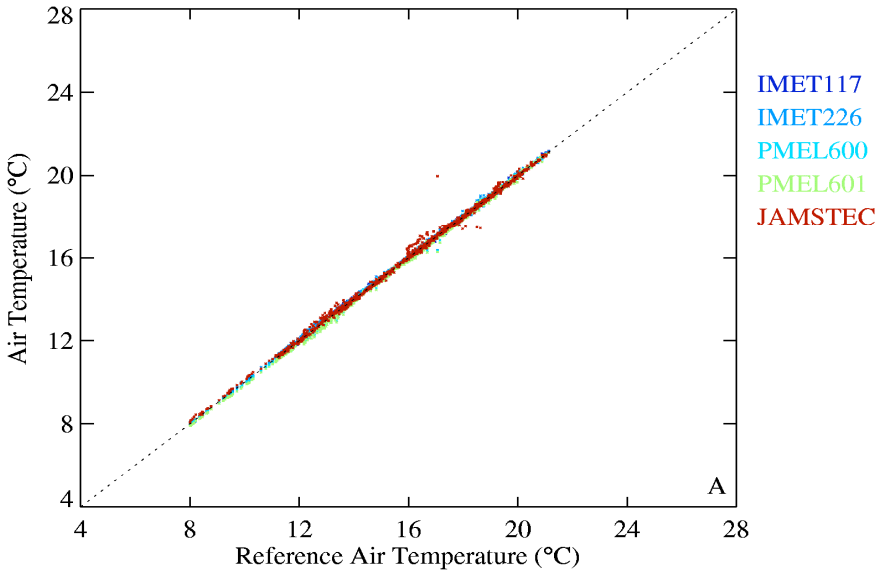
Air Temperature (°C)
Reference Air Temperature (°C)
A
IMET117
IMET226
PMEL600
PMEL601
JAMSTEC

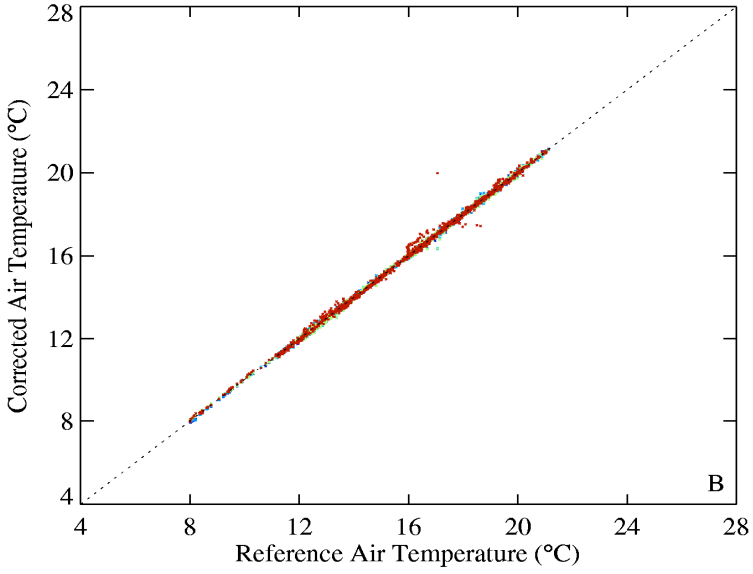
Corrected Air Temperature (°C)
Reference Air Temperature (°C)
B

Figure 15

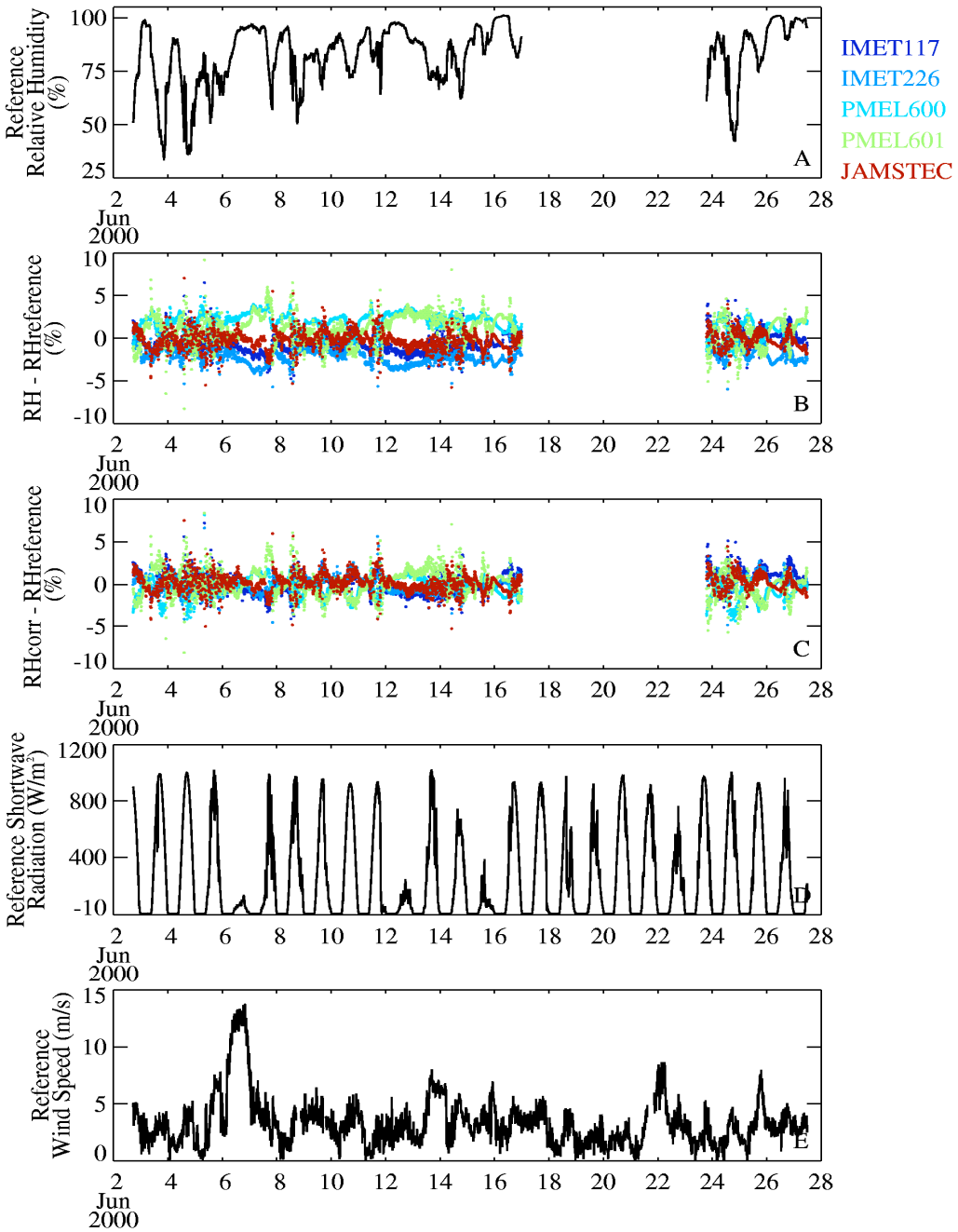
Reference Relative Humidity (%)
100
75
50
25
A
IMET117
IMET226
PMEL600
PMEL601
JAMSTEC
2 4 6 8 10 12 14 16 18 20 22 24 26 28
Jun 2000
RH - RHreference (%)
10
5
0
-5
-10
B
RHcorr - RHreference (%)
C
Reference Shortwave Radiation (W/m²)
1200
800
400
-10
D
Reference Wind Speed (m/s)
15
10
5
0
E

Figure 16

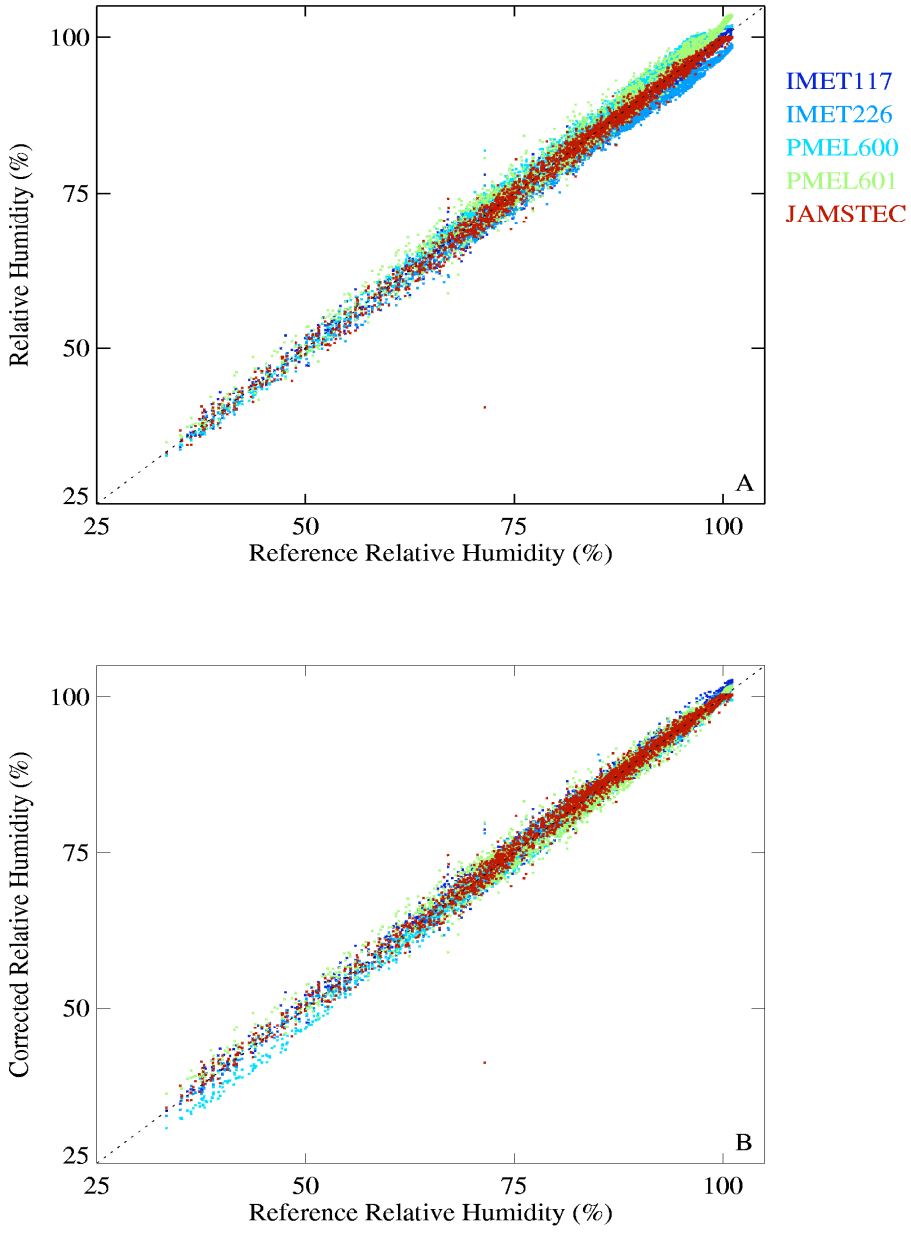
100
75
50
25
Relative Humidity (%)
25
50
75
100
Reference Relative Humidity (%)
A
IMET117
IMET226
PMEL600
PMEL601
JAMSTEC
100
75
50
25
Corrected Relative Humidity (%)
25
50
75
100
Reference Relative Humidity (%)
B

Figure 17

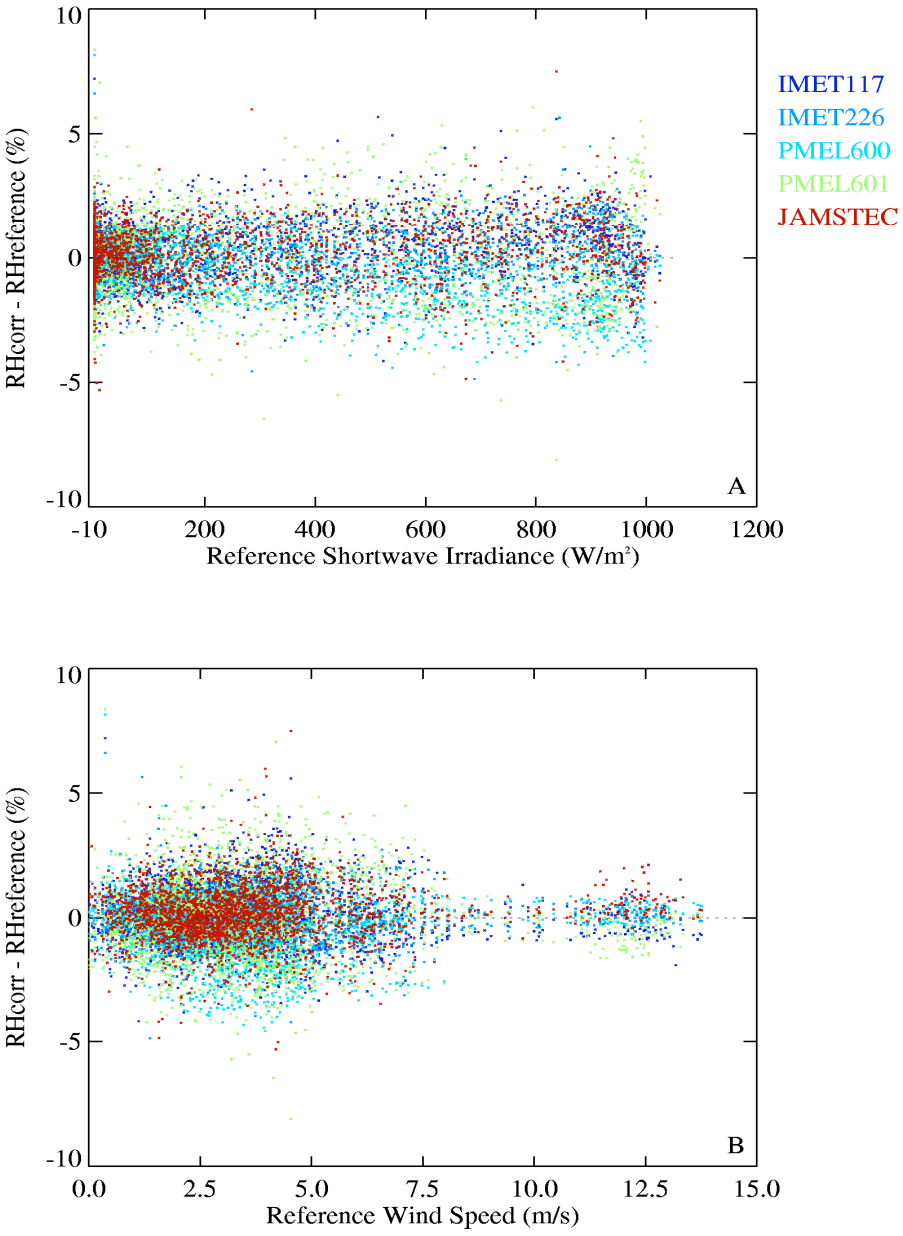
10
5
0
-5
-10
RHcorr - RHreference (%)
-10
200
400
600
800
1000
1200
Reference Shortwave Irradiance (W/m²)
A
IMET117
IMET226
PMEL600
PMEL601
JAMSTEC
10
5
0
-5
-10
RHcorr - RHreference (%)
0.0
2.5
5.0
7.5
10.0
12.5
15.0
Reference Wind Speed (m/s)
B

Figure 18

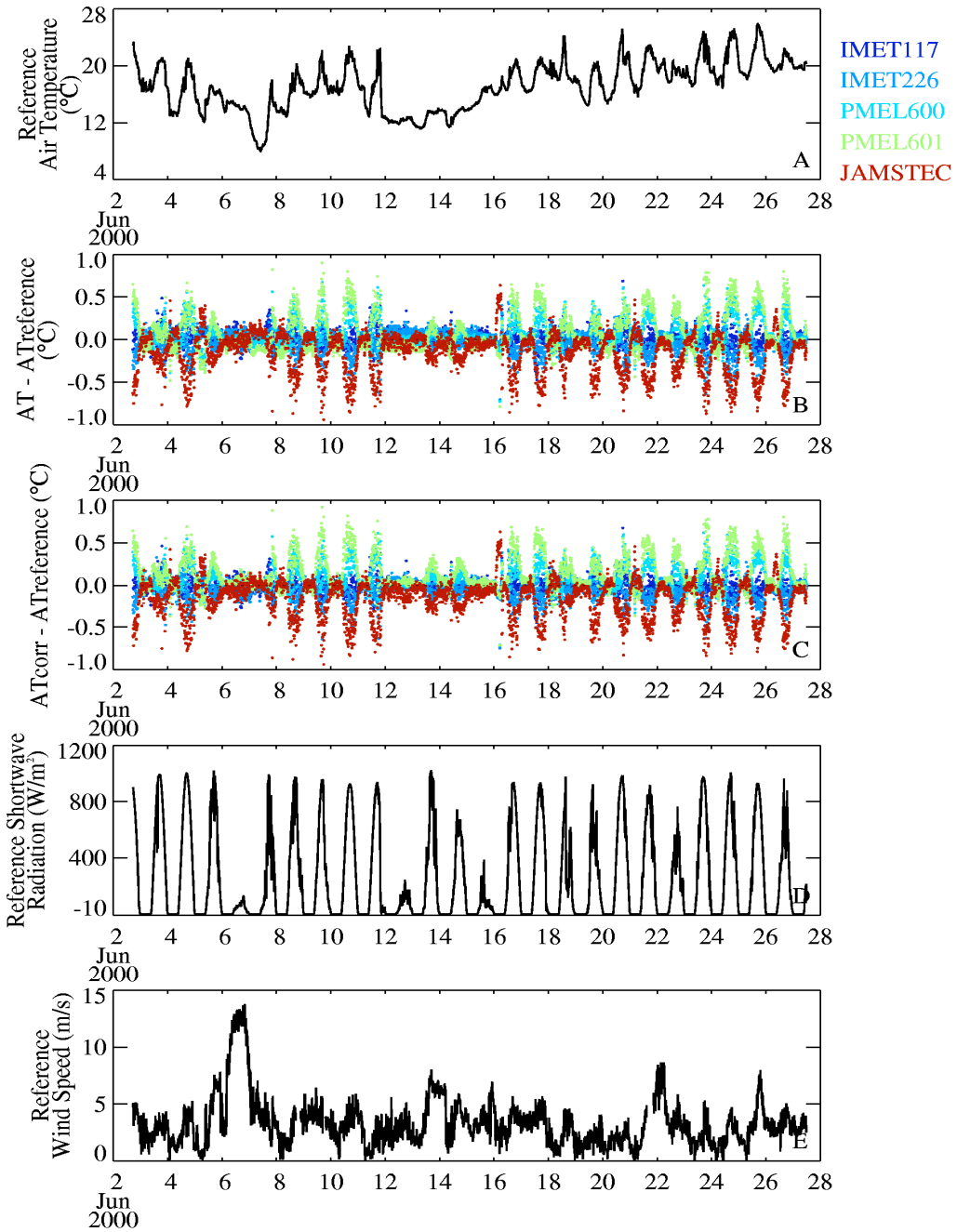
Reference Air Temperature (°C)
28
20
12
4
A
IMET117
IMET226
PMEL600
PMEL601
JAMSTEC
2 4 6 8 10 12 14 16 18 20 22 24 26 28
Jun 2000
AT - ATreference (°C)
1.0
0.5
0.0
-0.5
-1.0
B
ATcorr - ATreference (°C)
C
Reference Shortwave Radiation (W/m²)
1200
800
400
-10
D
Reference Wind Speed (m/s)
15
10
5
0
E

Figure 19

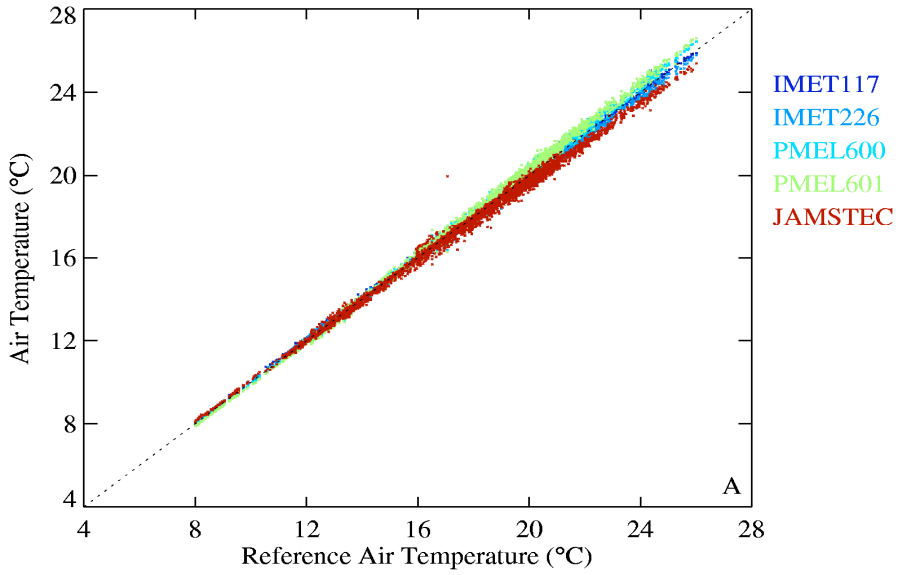
Air Temperature (°C)
Reference Air Temperature (°C)
A
IMET117
IMET226
PMEL600
PMEL601
JAMSTEC

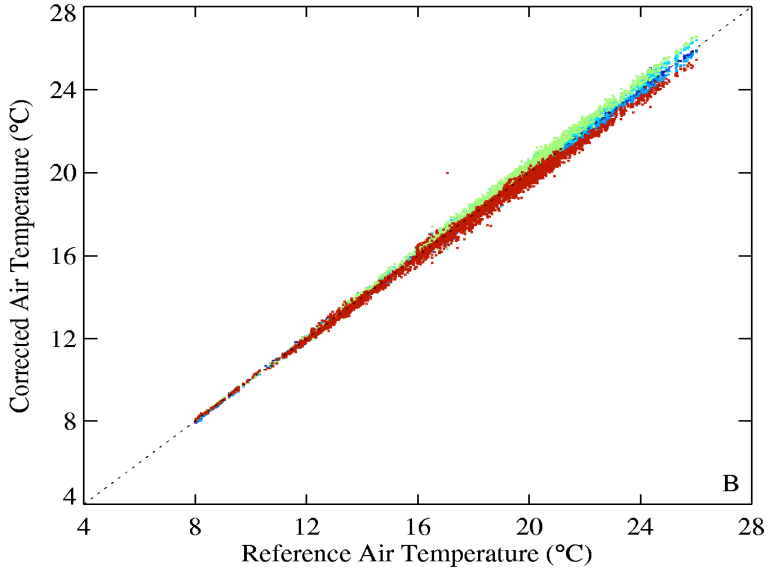
Corrected Air Temperature (°C)
Reference Air Temperature (°C)
B

Figure 20

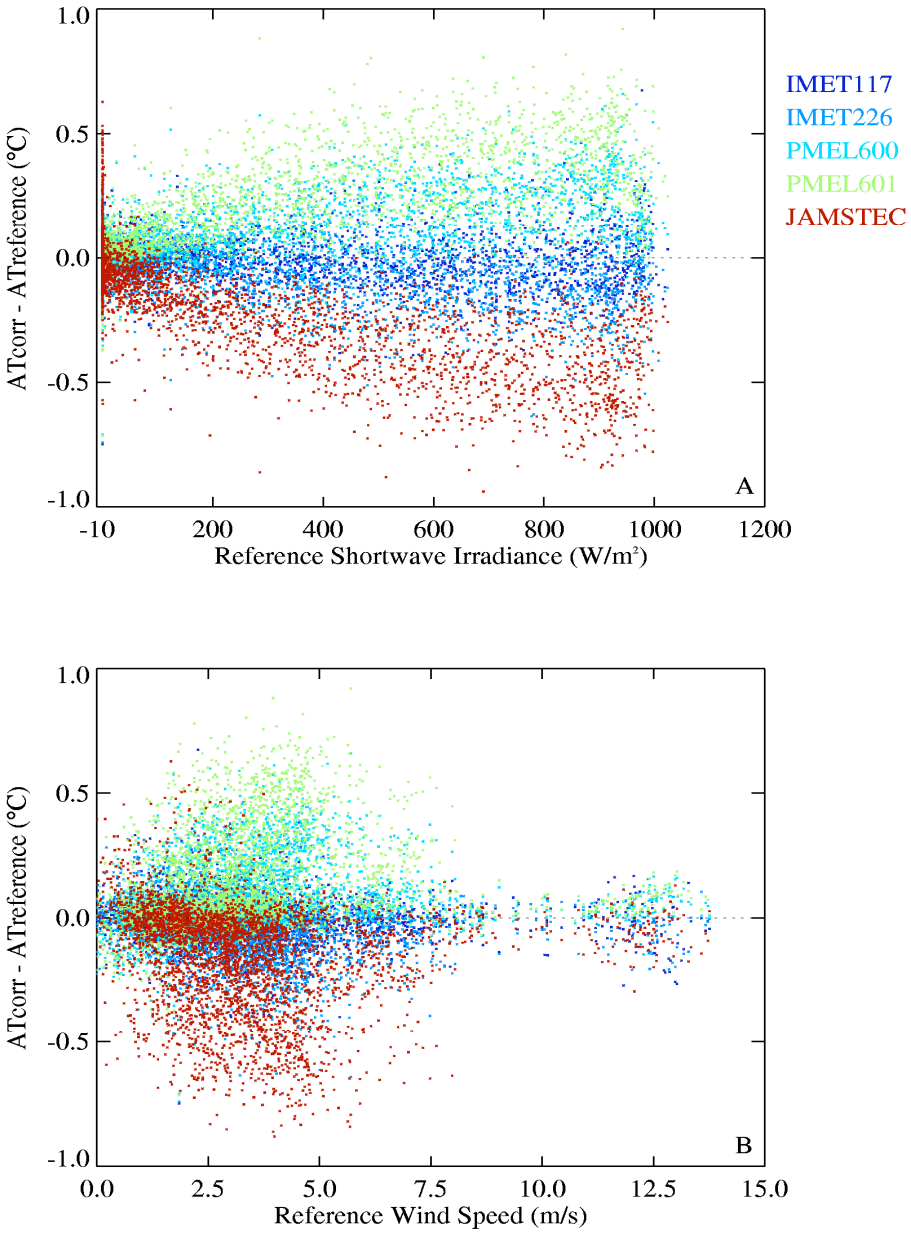
1.0
0.5
0.0
-0.5
-1.0
ATcorr - ATreference (°C)
-10
200
400
600
800
1000
1200
Reference Shortwave Irradiance (W/m²)
A
IMET117
IMET226
PMEL600
PMEL601
JAMSTEC
1.0
0.5
0.0
-0.5
-1.0
ATcorr - ATreference (°C)
0.0
2.5
5.0
7.5
10.0
12.5
15.0
Reference Wind Speed (m/s)
B

Figure 21

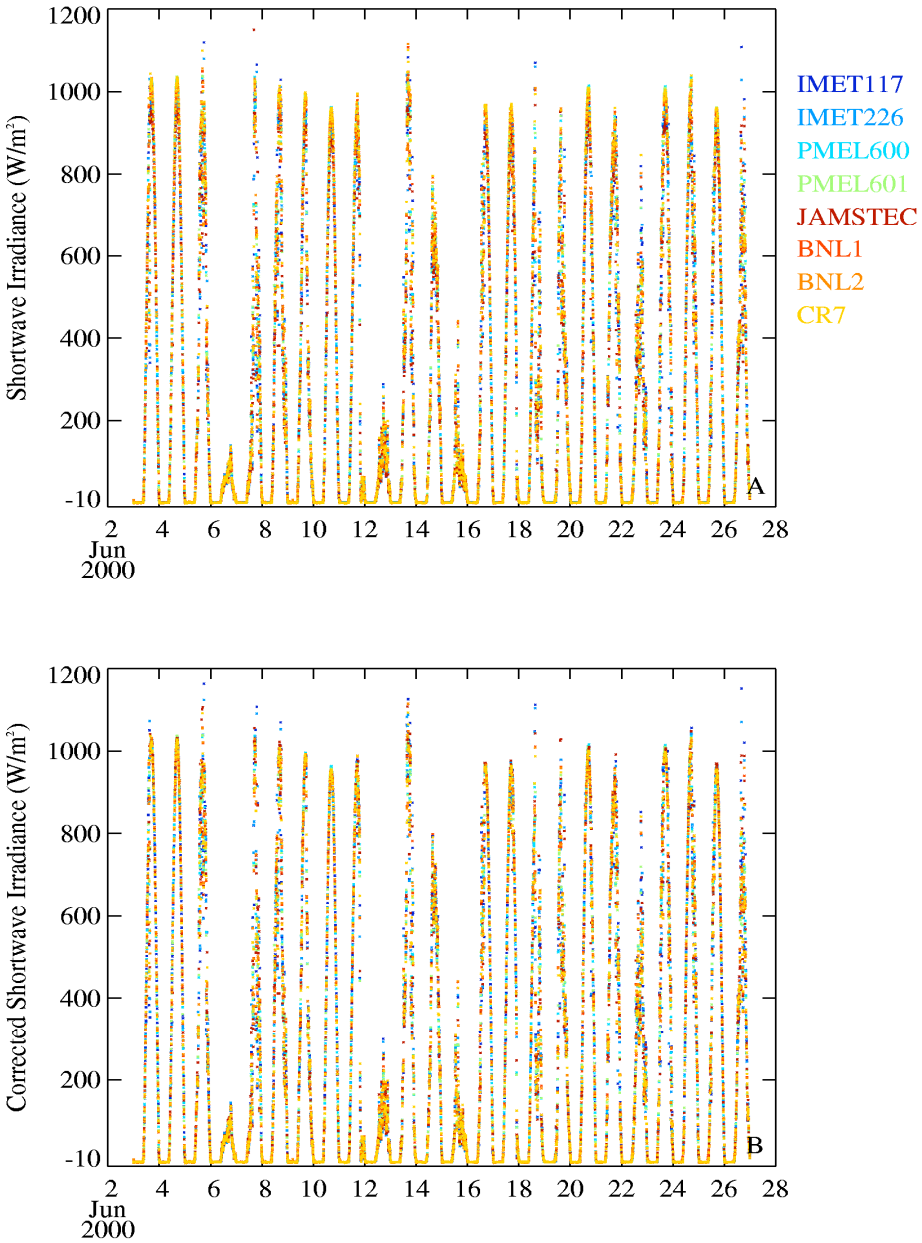
Shortwave Irradiance (W/m²)
Corrected Shortwave Irradiance (W/m²)
1200
1000
800
600
400
200
-10
2
4
6
8
10
12
14
16
18
20
22
24
26
28
Jun
2000
A
B
IMET117
IMET226
PMEL600
PMEL601
JAMSTEC
BNL1
BNL2
CR7

Figure 22

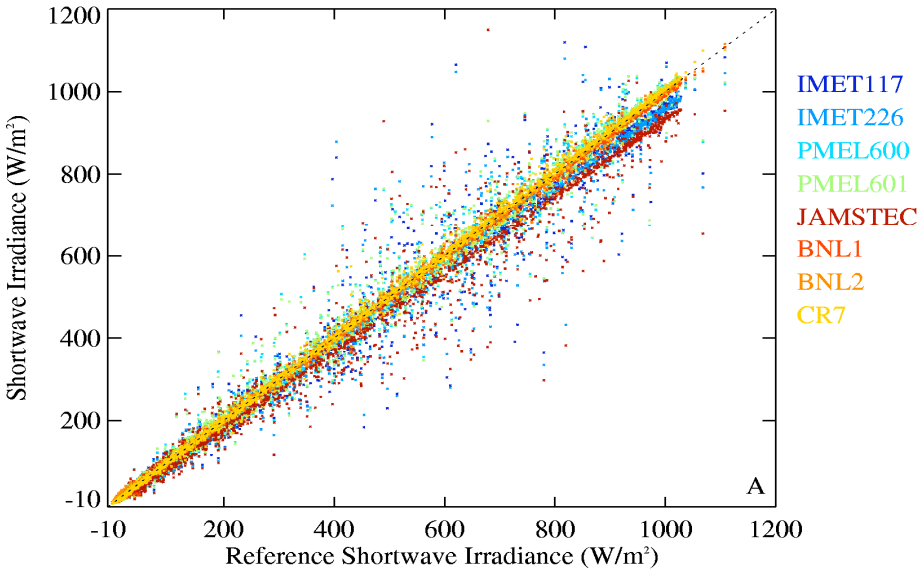
Shortwave Irradiance (W/m²)
Reference Shortwave Irradiance (W/m²)
1200
1000
800
600
400
200
-10
-10
200
400
600
800
1000
1200
A
IMET117
IMET226
PMEL600
PMEL601
JAMSTEC
BNL1
BNL2
CR7

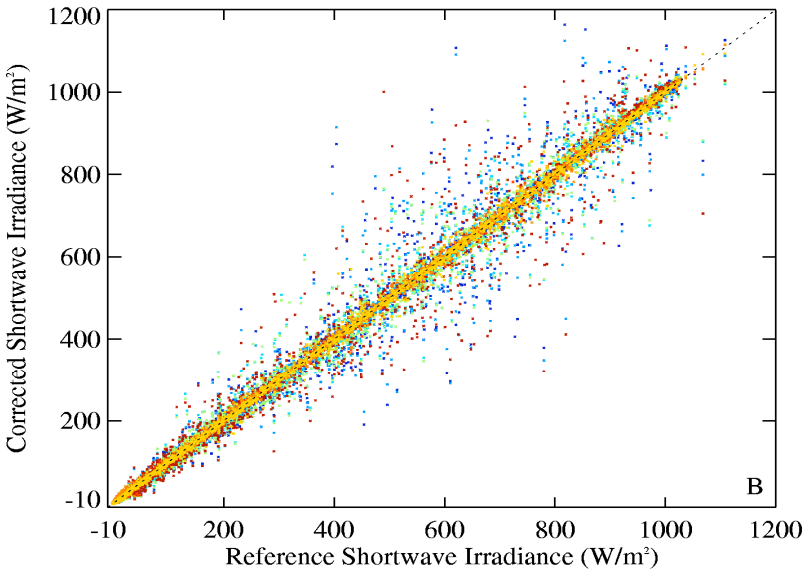
Corrected Shortwave Irradiance (W/m²)
Reference Shortwave Irradiance (W/m²)
1200
1000
800
600
400
200
-10
-10
200
400
600
800
1000
1200
B

Figure 23

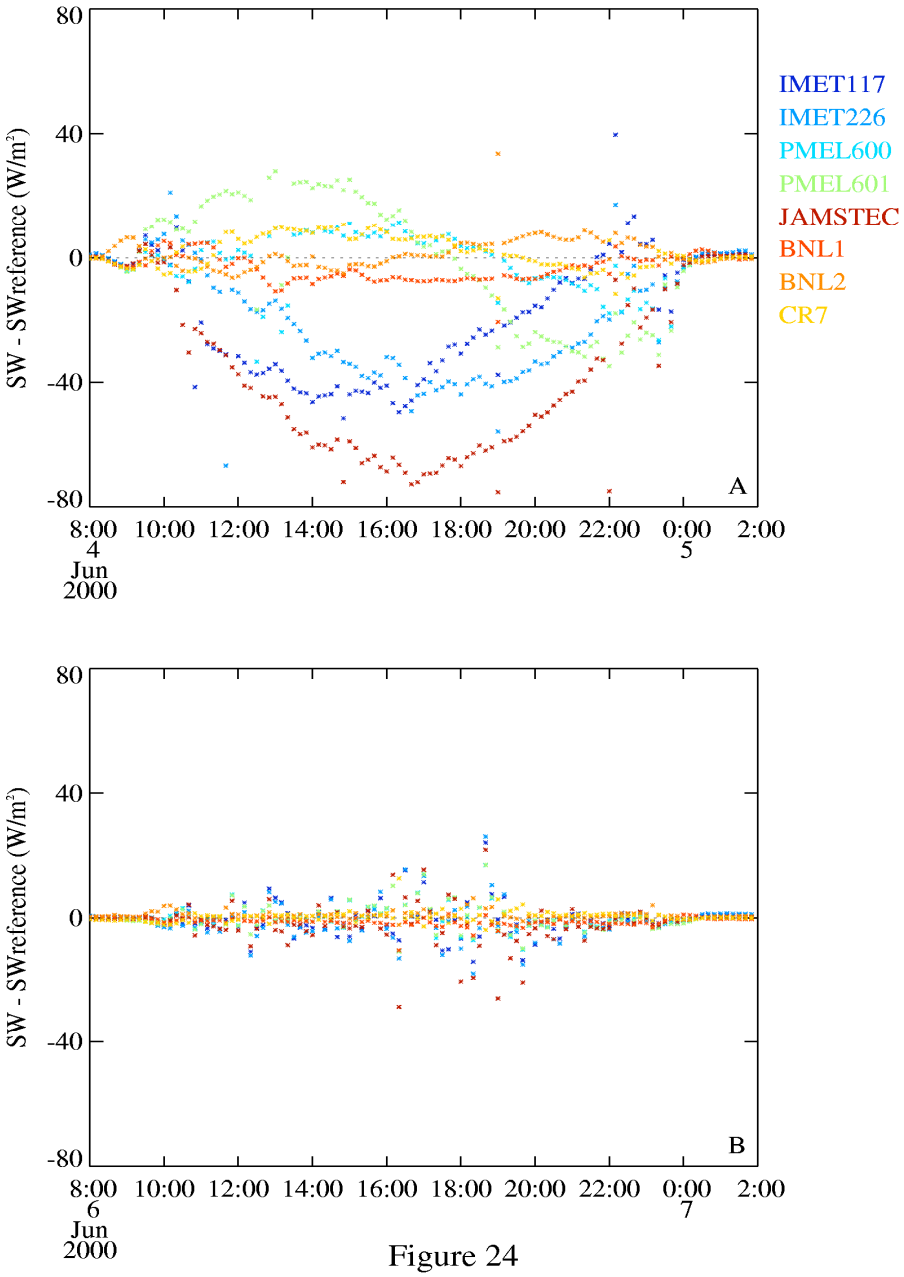
80
40
0
-40
-80
SW - SWreference (W/m²)
IMET117
IMET226
PMEL600
PMEL601
JAMSTEC
BNL1
BNL2
CR7
A
8:00
10:00
12:00
14:00
16:00
18:00
20:00
22:00
0:00
2:00
4
Jun
2000
5
B
6
Jun
2000
7

Figure 24

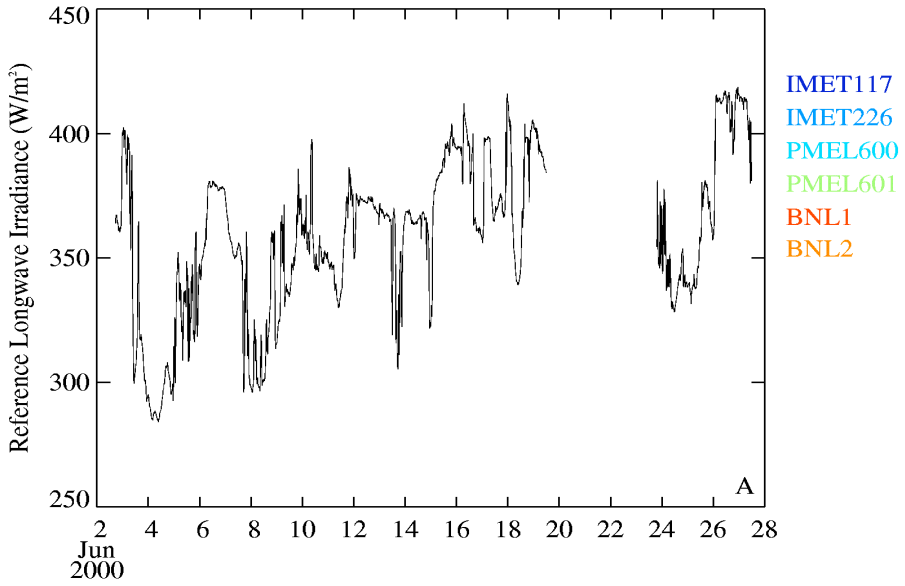
Reference Longwave Irradiance (W/m²)
450
400
350
300
250
2
4
6
8
10
12
14
16
18
20
22
24
26
28
Jun
2000
A
IMET117
IMET226
PMEL600
PMEL601
BNL1
BNL2

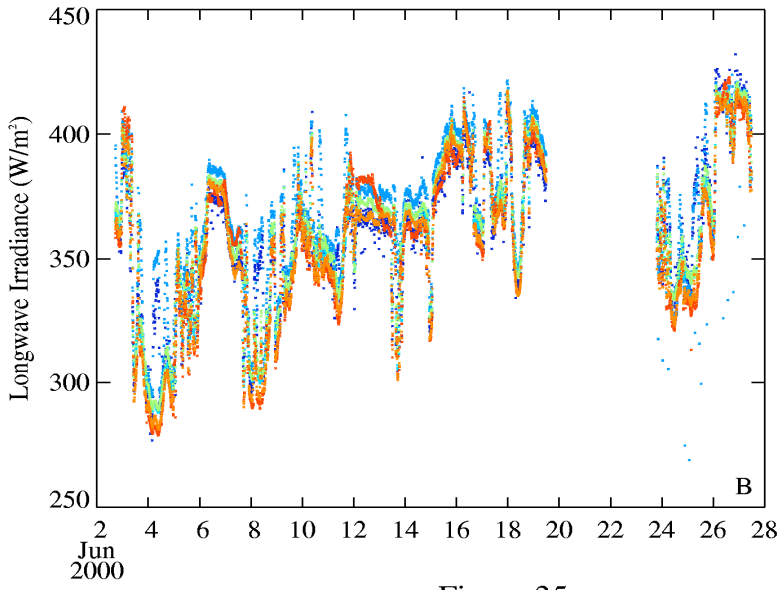
Longwave Irradiance (W/m²)
450
400
350
300
250
2
4
6
8
10
12
14
16
18
20
22
24
26
28
Jun
2000
B

Figure 25

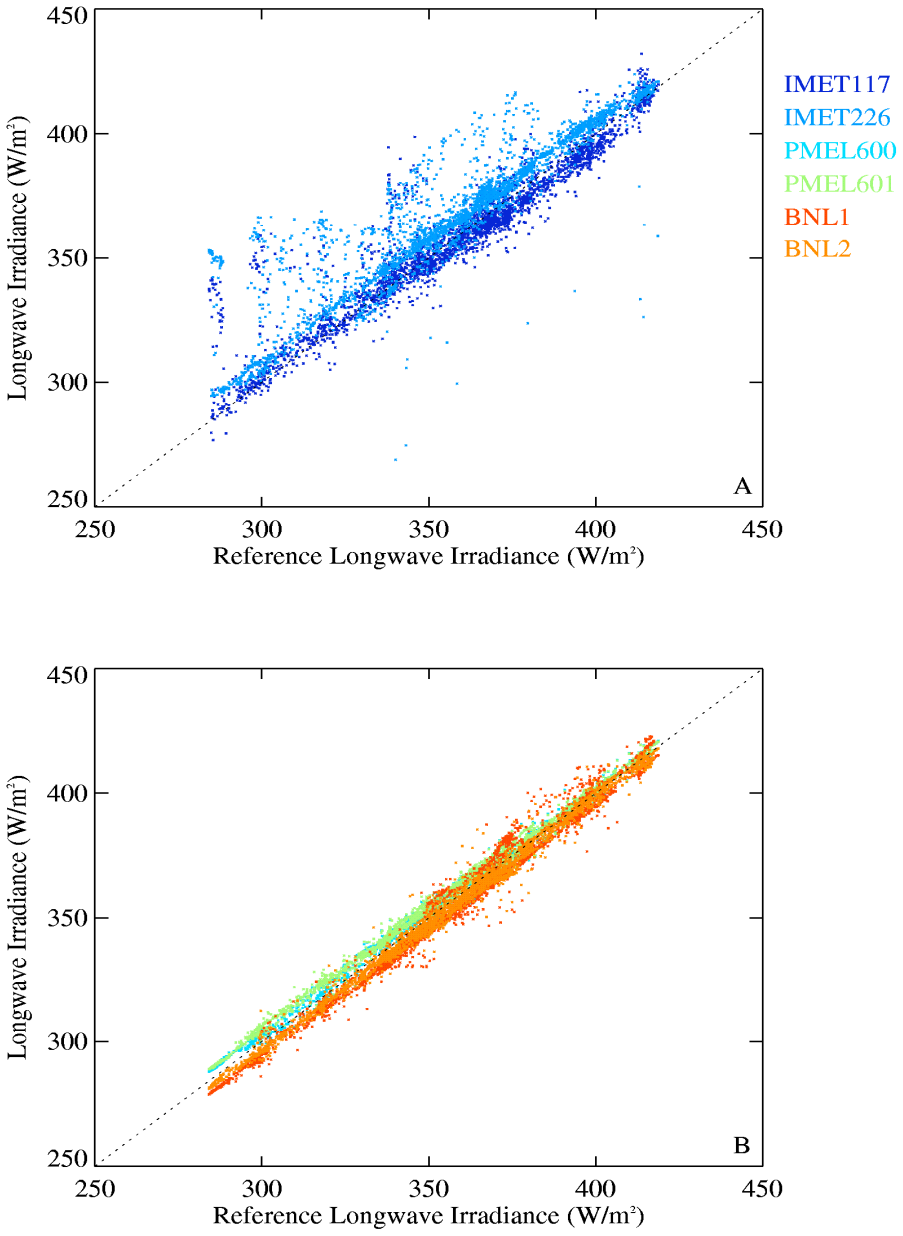
450
400
350
300
250
Longwave Irradiance (W/m²)
250
300
350
400
450
Reference Longwave Irradiance (W/m²)
A
IMET117
IMET226
PMEL600
PMEL601
BNL1
BNL2
450
400
350
300
250
Longwave Irradiance (W/m²)
250
300
350
400
450
Reference Longwave Irradiance (W/m²)
B

Figure 26

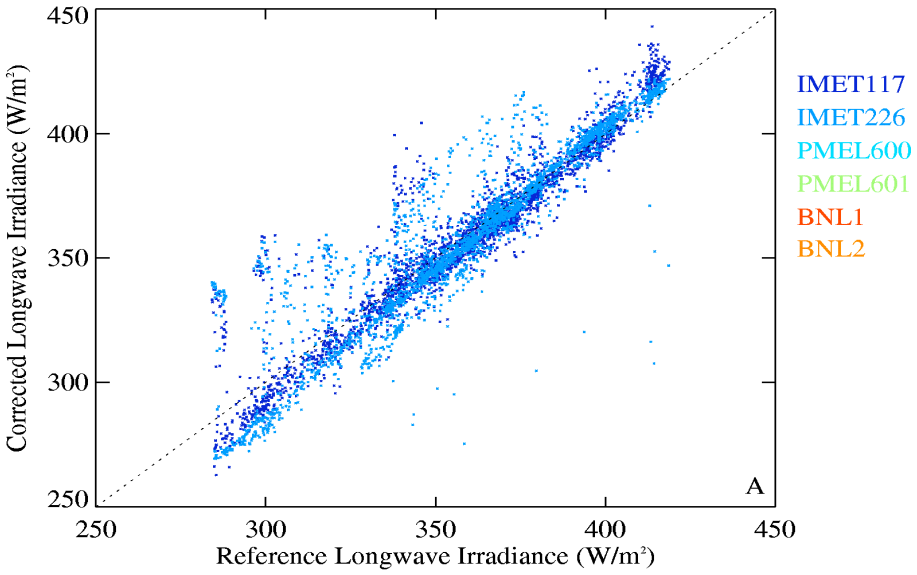
450
400
350
300
250
250
300
350
400
450
Corrected Longwave Irradiance (W/m²)
Reference Longwave Irradiance (W/m²)
A
IMET117
IMET226
PMEL600
PMEL601
BNL1
BNL2

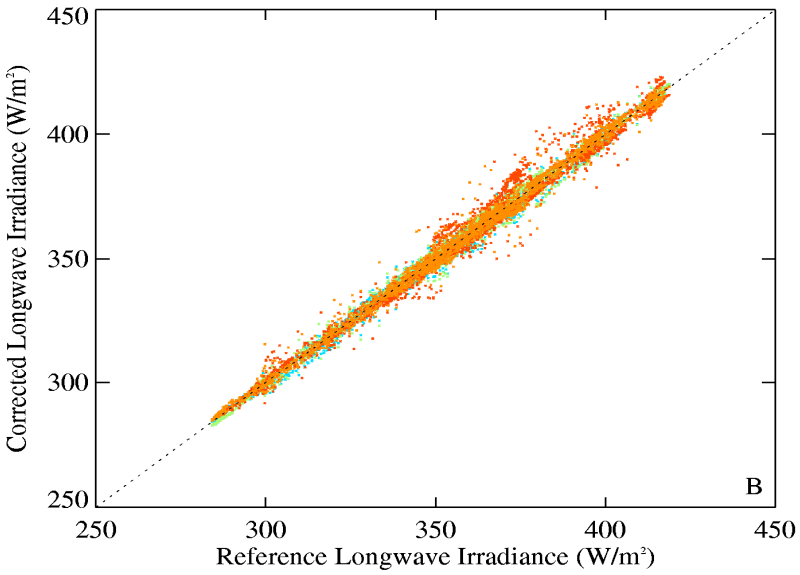
450
400
350
300
250
250
300
350
400
450
Corrected Longwave Irradiance (W/m²)
Reference Longwave Irradiance (W/m²)
B

Figure 27

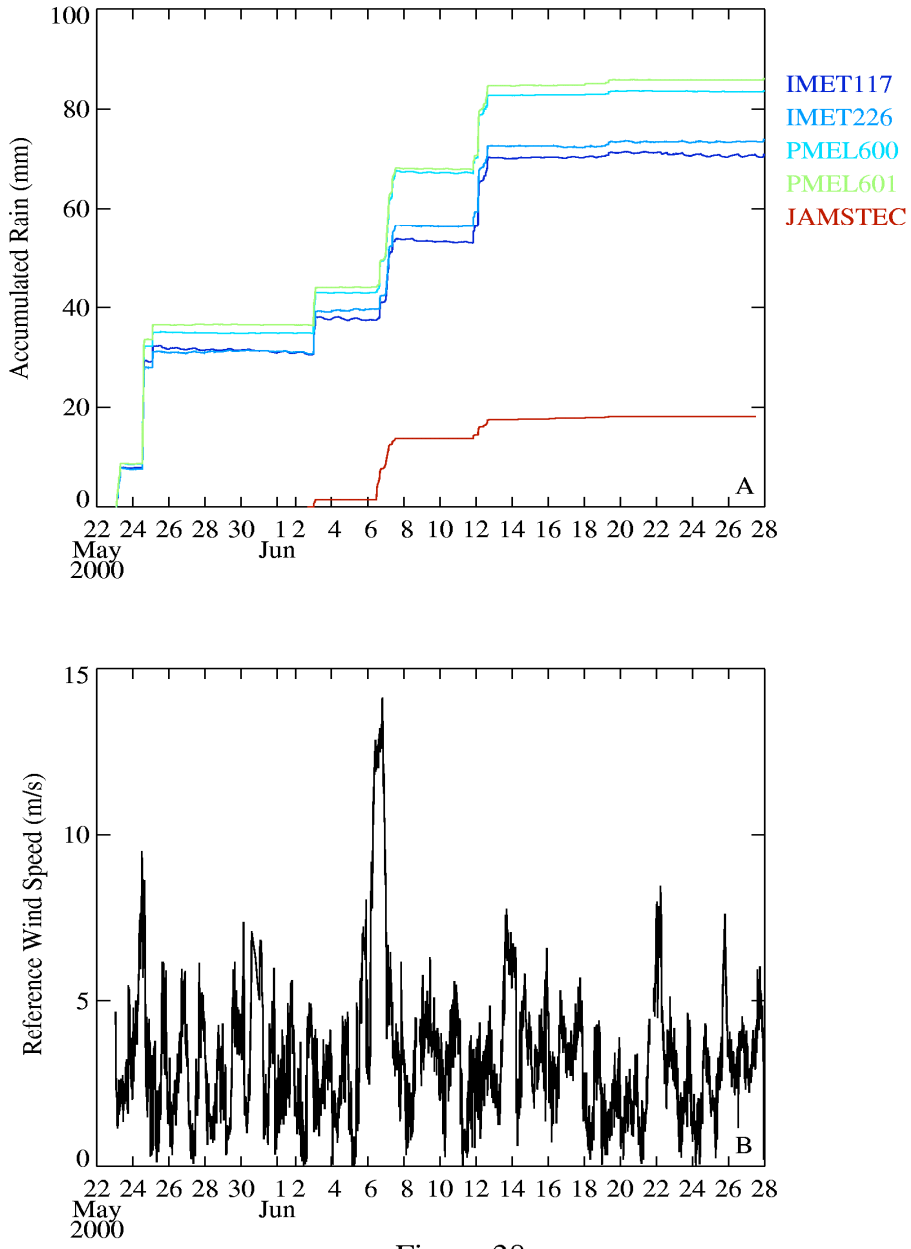
Accumulated Rain (mm)
100
80
60
40
20
0
22 24 26 28 30 1 2 4 6 8 10 12 14 16 18 20 22 24 26 28
May
Jun
2000
A
IMET117
IMET226
PMEL600
PMEL601
JAMSTEC
Reference Wind Speed (m/s)
15
10
5
0
22 24 26 28 30 1 2 4 6 8 10 12 14 16 18 20 22 24 26 28
May
Jun
2000
B

Figure 28

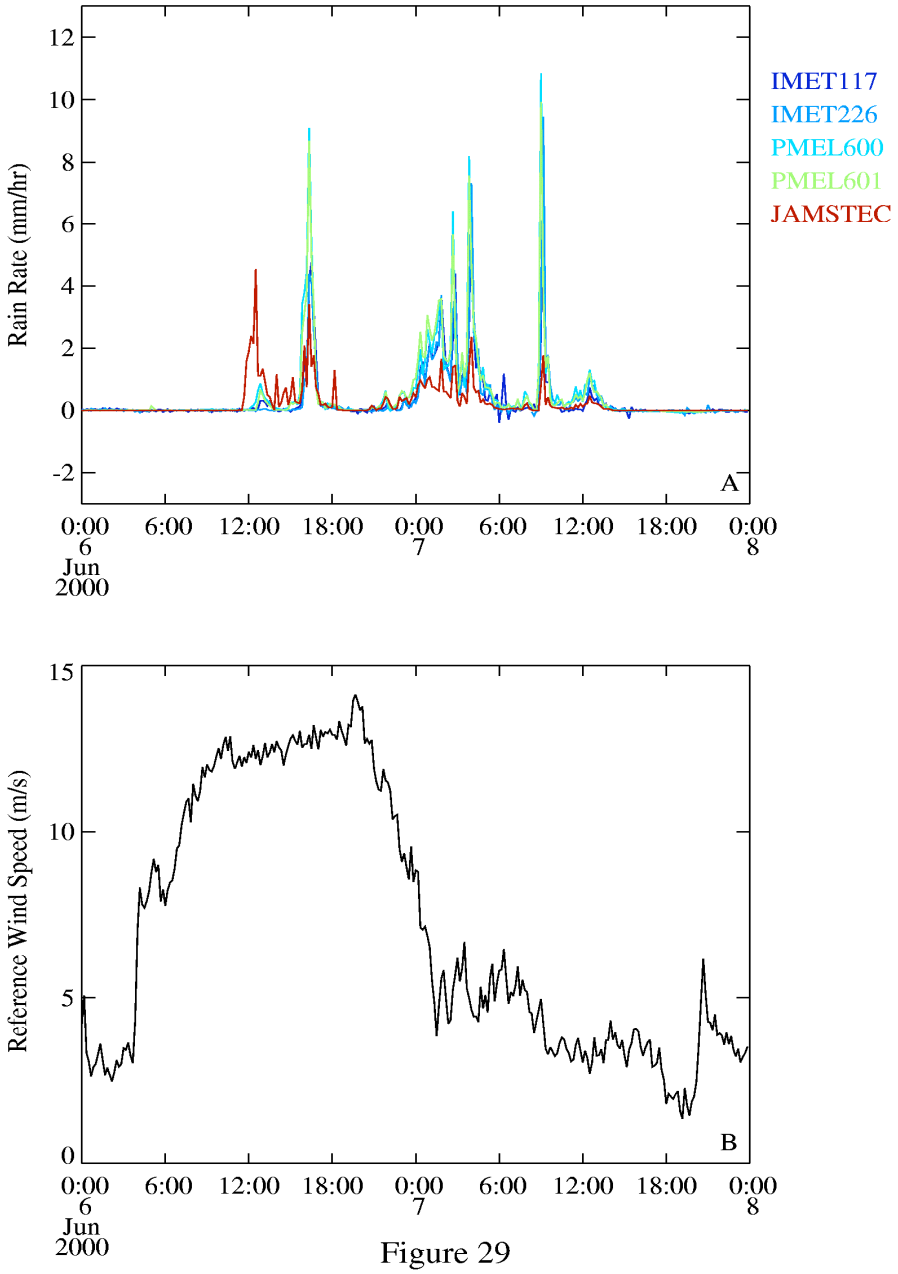
Rain Rate (mm/hr)
12
10
8
6
4
2
0
-2
A
IMET117
IMET226
PMEL600
PMEL601
JAMSTEC
0:00
6
Jun
2000
6:00
12:00
18:00
0:00
7
6:00
12:00
18:00
0:00
8
Reference Wind Speed (m/s)
15
10
5
0
B
0:00
6
Jun
2000
6:00
12:00
18:00
0:00
7
6:00
12:00
18:00
0:00
8

Figure 29

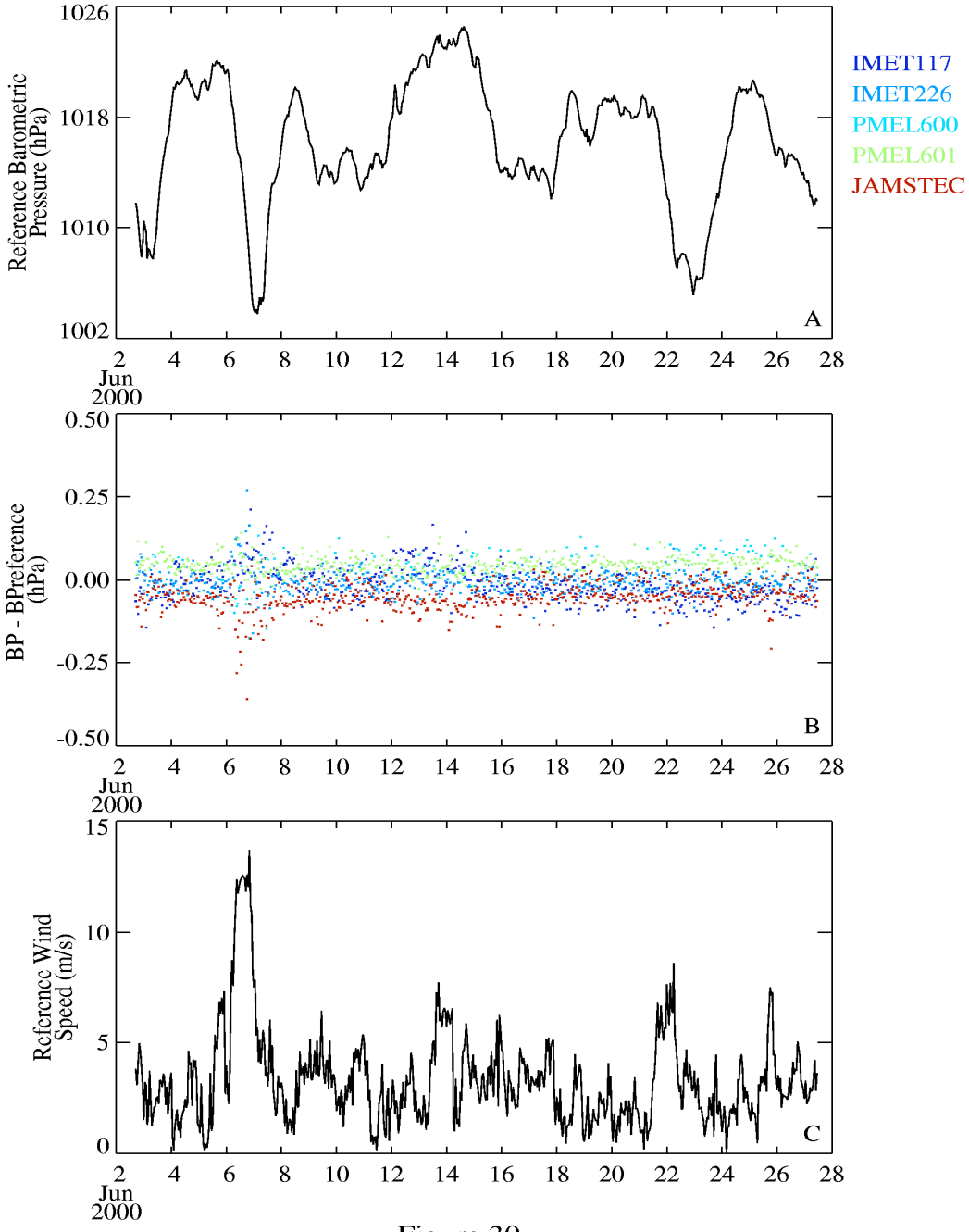
Reference Barometric Pressure (hPa)
1026
1018
1010
1002
A
2 4 6 8 10 12 14 16 18 20 22 24 26 28
Jun
2000
IMET117
IMET226
PMEL600
PMEL601
JAMSTEC
BP - BPreference (hPa)
0.50
0.25
0.00
-0.25
-0.50
B
2 4 6 8 10 12 14 16 18 20 22 24 26 28
Jun
2000
Reference Wind Speed (m/s)
15
10
5
0
C
2 4 6 8 10 12 14 16 18 20 22 24 26 28
Jun
2000

Figure 30